

# Development of Thioaryl-based Matrix Metalloproteinase-12 Inhibitors with Alternative Zinc-Binding Groups: Synthesis, Potentiometric, NMR and Crystallographic Studies

Elisa Nuti,<sup>a</sup> Doretta Cuffaro,<sup>a</sup> Elisa Bernardini,<sup>a,b</sup> Caterina Camodeca,<sup>a</sup> Laura Panelli,<sup>a</sup> Sílvia Chaves,<sup>b</sup> Lidia Ciccone,<sup>c,d</sup> Livia Tepshi,<sup>c</sup> Laura Vera,<sup>c,e</sup> Elisabetta Orlandini,<sup>f</sup> Susanna Nencetti,<sup>a</sup> Enrico A. Stura,<sup>c</sup> M. Amélia Santos,<sup>b</sup> Vincent Dive,<sup>c</sup> and Armando Rossello<sup>\*a</sup>

<sup>a</sup> *Dipartimento di Farmacia, Università di Pisa, Via Bonanno 6, 56126 Pisa, Italy*

<sup>b</sup> *Centro de Química Estrutural, Instituto Superior Técnico, Universidade de Lisboa, Av. Rovisco Pais 1, 1049-001 Lisboa, Portugal*

<sup>c</sup> *CEA, Institut des Sciences du Vivant Frédéric Joliot, Service d'Ingénierie Moléculaire des Protéines (SIMOPRO), Université Paris-Saclay, Gif-sur-Yvette, 91190*

<sup>d</sup> *Synchrotron SOLEIL, L'Orme des Merisiers, Saint-Aubin, BP 48, 91192 Gif-sur-Yvette, France*

<sup>e</sup> *Laboratory of Biomolecular Research, Division of Biology and Chemistry, Paul Scherrer Institute, 5232 Villigen, Switzerland*

<sup>f</sup> *Dipartimento di Scienze della Terra, Università di Pisa, via Santa Maria 53, 56126 Pisa, Italy*

\*Corresponding Author: Armando Rossello, phone: +39 0502219562; e-mail: [armando.rossello@farm.unipi.it](mailto:armando.rossello@farm.unipi.it)

## Abstract

Matrix metalloproteinase-12 (MMP-12) selective inhibitors could play a role in the treatment of lung inflammatory and cardiovascular diseases. In the present study, the previously reported 4-methoxybiphenylsulfonyl hydroxamate and carboxylate-based inhibitors (**1b** and **2b**) were modified to enhance their selectivity for MMP-12. In the newly synthesized thioaryl derivatives, the nature of the

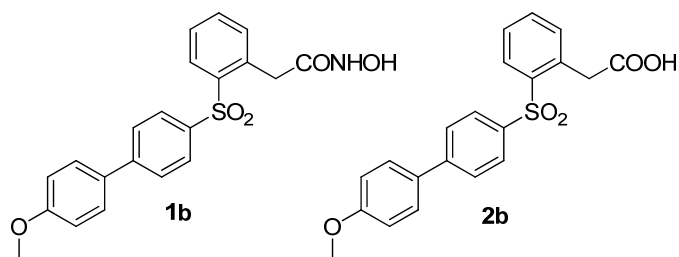
zinc binding group (ZBG) and the sulfur oxidation state were changed. Biological assays carried out *in vitro* on human MMPs with the resulting compounds led to identify a sulfide, **4a**, bearing a *N*-1-hydroxypiperidine-2,6-dione (HPD) group as new ZBG. **4a** is a promising hit compound since it displayed a nanomolar affinity for MMP-12 with a marked selectivity over MMP-9, MMP-1 and MMP-14. Solution complexation studies with  $\text{Zn}^{2+}$  were performed to characterize the chelating abilities of the new compounds and confirmed the bidentate binding mode of HPD derivatives. X-ray crystallography studies using MMP-12 and MMP-9 catalytic domains were carried out to rationalize the biological results.

## 1. Introduction

Matrix metalloproteinases (MMPs), also designated matrixins, constitute a family of more than 20 structurally and functionally related metalloenzymes. Through the hydrolysis of different components of the extracellular matrix (ECM), these proteinases play a pivotal role in many biological processes, such as embryonic development, tissue remodeling, wound healing, and angiogenesis. Their expression is finely regulated at many levels (transcription, activation, inhibition) while unregulated profiles were found to be associated with pathological conditions. It is for this reason that these enzymes represent a real interest for researchers as therapeutic targets. In fact, they are involved in the pathogenesis of several serious and chronic diseases such as osteoarthritis, rheumatoid arthritis, vascular diseases and cancer metastasis.<sup>1</sup> MMPs are zinc-dependent metalloenzymes. The conserved catalytic domain contains a catalytic  $\text{Zn}^{2+}$  ion, a structural  $\text{Zn}^{2+}$  ion, and one to three structural  $\text{Ca}^{2+}$  ions necessary for enzyme stability.<sup>2</sup> In general, a small molecule MMP inhibitor (MMPI) consists of a backbone and a zinc-binding group (ZBG). The backbone is a classic drug-like structure that interacts with the protein through non-covalent bonds while the ZBG is a group able to chelate the catalytic zinc ion. Widely utilized ZBGs include: hydroxamic acids, carboxylic acids, pyrimidinetriones, thiols and phosphinates.<sup>3</sup>

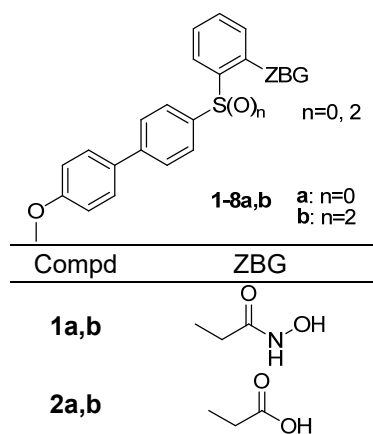
Among them, the most used is the hydroxamate group due to its excellent chelating properties.<sup>4</sup> It coordinates the catalytic  $Zn^{2+}$  in a bidentate fashion to form a complex with distorted trigonal bipyramidal geometry. Strong affinity for  $Zn^{2+}$  is often accompanied by poor selectivity. In addition, the hydroxamate group is characterized by a well-known hydrolytic susceptibility which often precludes the clinical use of hydroxamate-based MMPiS.<sup>5</sup> Carboxylate-based MMPiS also present some drawbacks related to a lower potency and higher plasma protein binding<sup>6</sup> than their hydroxamate analogues which often cause a reduced bioavailability and *in vivo* efficacy.<sup>7</sup>

Among all MMPs, gelatinases (MMP-2 and -9) and metalloelastase (MMP-12) have a fundamental role in the development of different and relevant pathologies. MMP-2 and MMP-9 are particularly involved in cancer pathogenesis and progression.<sup>8</sup> MMP-12 is mainly produced by macrophages and it is involved in acute and chronic pulmonary inflammatory diseases associated with intense airway remodeling, such as chronic obstructive pulmonary disease (COPD) and emphysema.<sup>9</sup> Moreover, MMP-12 plays an important role in the development of aneurysms and atherosclerosis.<sup>10</sup> Thus, the development of MMP-12 selective inhibitors could be useful for the treatment of lung inflammatory and cardiovascular diseases. So far, only a few inhibitors highly selective for MMP-12 have been described.<sup>11</sup> We previously reported the design and synthesis of a series of arylsulfone hydroxamates and carboxylates as potent MMP-12 inhibitors.<sup>12</sup> Among these, in the present study we have selected to optimize the 4-methoxybiphenylsulfonyl derivatives (**1b** and **2b**, Figure 1) with the aim of improving their selectivity profiles. The compound's backbone was left unchanged, given its good fit into the channel-like S1' pocket of MMP-12, but the ZBG was varied. This strategy is supported by recent studies that have shown that also the ZBG is important in determining the selectivity of inhibition toward a specific MMP.<sup>13,14</sup>



**Figure 1.** Structure of the previously reported MMP-12 inhibitors.

We started with the synthesis of new diaryl sulfone derivatives with ZBGs other than hydroxamic acids (compounds **3-8b**, Chart 1) to evaluate how the potency and selectivity for MMP-12 is affected by the ZBG. We then synthesized their sulfide analogues (compounds **1-8a**, Chart 1) to understand how the oxidation state of the sulfur atom impacts on the binding of the inhibitor to MMP-12. The absence of the oxygen atoms would reduce the ability to establish H-bonds with the enzyme in proximity of the catalytic zinc, but also remove steric constraints that might prevent the spatial optimization of the compound in the S1' pocket. The inhibitory activities of the new thioaryl-based MMP-12 inhibitors were tested *in vitro* by using recombinant MMPs. Solution equilibrium Zn(II)-complexation studies were performed by potentiometric and spectroscopic (NMR) techniques to characterize the chelating abilities of the new compounds and X-ray crystallography studies were used to rationalize the biological results.



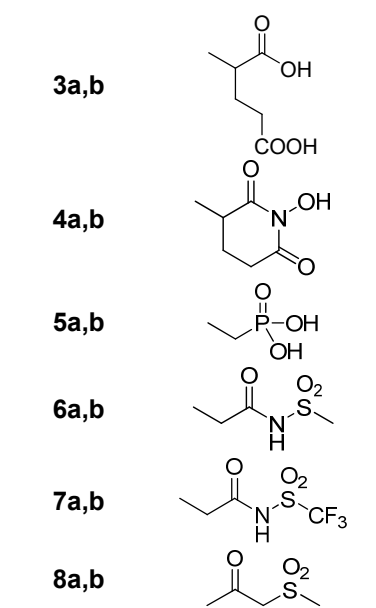


**Chart 1**

## 2. Results and discussion.

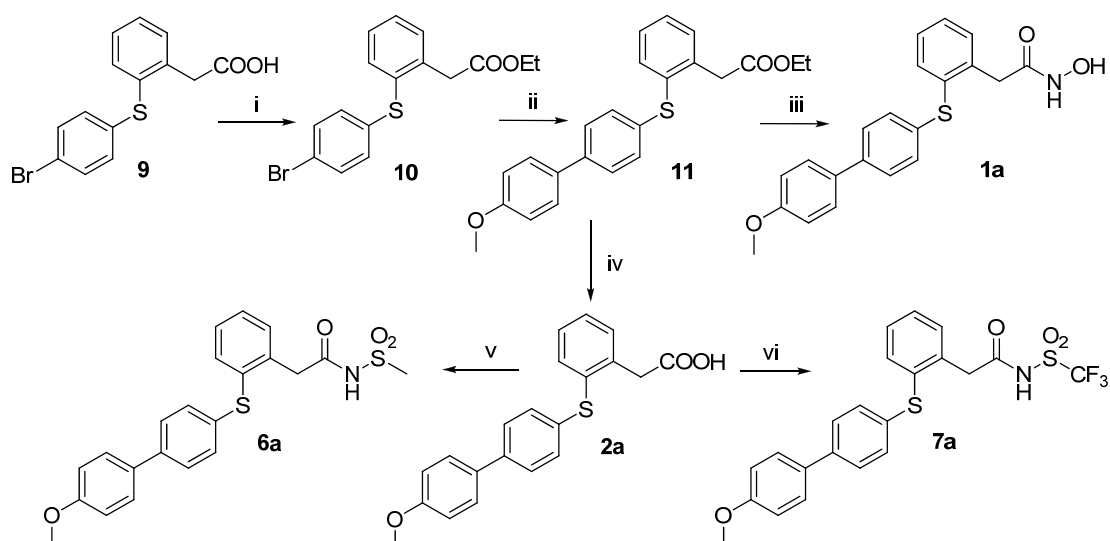
### 2.1. Design of MMP-12 inhibitors with new ZBGs.

With the aim of developing new thioaryl-based MMP-12 inhibitors with improved selectivity and hydrolytic stability with respect to **1b**, we selected different functional groups to be used as ZBGs alternative to the hydroxamic acid. Firstly, a *N*-1-hydroxypiperidine-2,6-dione (HPD) moiety was chosen for derivatives **4a,b** based on previous results with compounds containing a similar non-classical ZBG (1-hydroxypiperazine-2,6-dione) which were effective inhibitors of MMPs, with activities in the nanomolar range.<sup>15</sup> Novel ZBGs, namely hydroxypyridinones (HOPOs) and pyrones have also been shown to be effective for the design of MMP inhibitors.<sup>16,17</sup> Due to its six-membered ring closure, the HPD moiety is likely to be more stable and better resistant to hydrolysis than hydroxamates. In derivatives **3a,b**, a dicarboxylic acid was taken in consideration as an alternative bidentate ZBG, given its promising results in previously described MMPIs that showed a good activity and selectivity for MMP-2 and -9 over MMP-1.<sup>18</sup> Then, three functional groups considered to be “soft binders” for the catalytic zinc ion were selected: a *N*-acylmethanesulfonamide (derivatives **6a,b**), a *N*-acyl(trifluoromethane)sulfonamide (derivatives **7a,b**) and a methylsulfonyl ethanone group (derivatives

**8a,b**). Finally, hydroxamic acid (**1a,b**), carboxylic acid (**2a,b**) and phosphonate (**5a,b**) derivatives were also prepared for comparison.

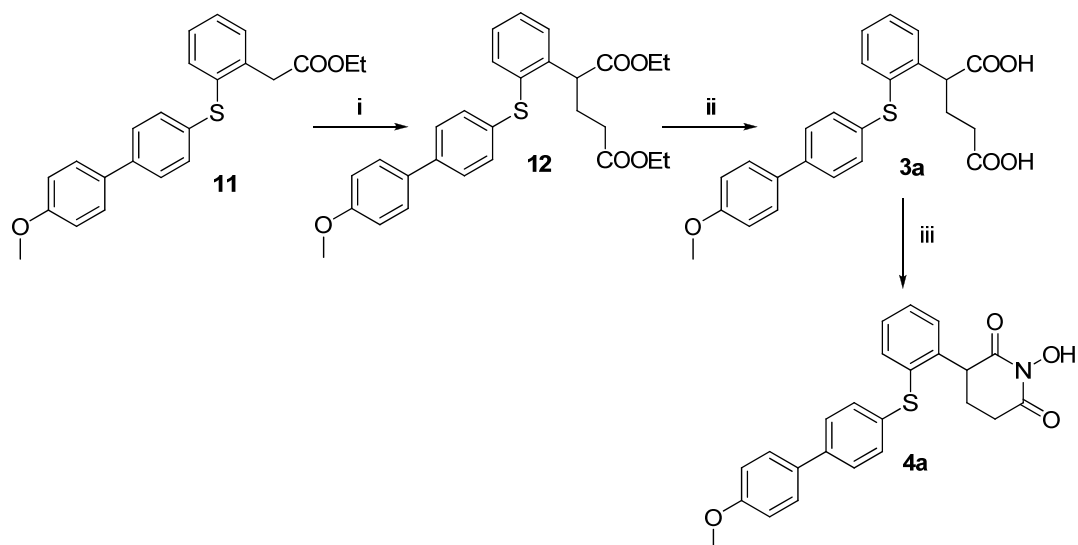
## 2.2. Chemistry.

Diarylsulfide derivatives **1a**, **2a**, **6a** and **7a** were prepared as reported in Scheme 1. The previously described, 2-(2-(4-bromophenylthio)phenyl)acetic acid **9**<sup>12</sup>, was protected as ethyl ester by treatment with thionyl chloride (SOCl<sub>2</sub>) in ethanol. This step was necessary to improve the subsequent cross-coupling reaction, which exhibited poor yield if conducted on carboxylic acid. A Palladium-catalyzed cross-coupling reaction (Suzuki conditions) of protected arylbromide **10** with 4-methoxyphenylboronic acid afforded biphenyl derivative **11**. The key intermediate **11** was converted to its corresponding hydroxamic acid **1a** by direct treatment with hydroxylamine hydrochloride (NH<sub>2</sub>OH HCl) and potassium hydroxide (KOH) in a mixture of methanol/dioxane. Basic hydrolysis of ester **11** by NaOH in dioxane afforded carboxylic acid **2a**, in quantitative yields. Subsequently, **2a** was converted into sulfonamides **6a** and **7a** by condensation with methanesulfonamide (CH<sub>3</sub>SO<sub>2</sub>NH<sub>2</sub>) or trifluoromethanesulfonamide (CF<sub>3</sub>SO<sub>2</sub>NH<sub>2</sub>), respectively, in the presence of *N*-(3-dimethylaminopropyl)-*N*'-ethylcarbodiimide (EDC) and 4-dimethylaminopyridine (DMAP) using dichloromethane as solvent.



**Scheme 1.** Synthesis of compounds **1a**, **2a**, **6a** and **7a**. Reagents and conditions: i)  $\text{SOCl}_2$ , EtOH, 60 °C, 4 h, 85%; ii) 4-methoxyphenylboronic acid,  $\text{Pd}(\text{PPh}_3)_4$ ,  $\text{Na}_2\text{CO}_3$ , toluene/EtOH, 100 °C, 2 h, 72%; iii)  $\text{NH}_2\text{OH HCl}$ , KOH, MeOH, 16 h, 88%; iv) NaOH 1N, dioxane, 16 h, quant.; v)  $\text{CH}_3\text{SO}_2\text{NH}_2$ , EDC, DMAP,  $\text{CH}_2\text{Cl}_2$ , 5 h, 55%; vi)  $\text{CF}_3\text{SO}_2\text{NH}_2$ , EDC, DMAP,  $\text{CH}_2\text{Cl}_2$ , 5 h, 82%.

The synthesis of dicarboxylic acid **3a** and *N*-hydroxypiperidin-dione **4a** is described in Scheme 2. The biphenyl-thioaryl ester **11** was alkylated by Michael addition, using ethyl acrylate and sodium hydride (NaH) in *t*-BuOH/DMF 4:1, to give diester **12**. The dicarboxylic acid **3a** was obtained by saponification with KOH solution of **12** and it was subsequently converted into the corresponding *N*-hydroxypiperidin-dione **4a**. This step was performed in THF, through a one-pot reaction, where the carboxylic groups have previously been activated by reacting with ethyl chloroformate, followed by treatment with hydroxylamine hydrochloride in basic methanol and THF.<sup>19</sup>



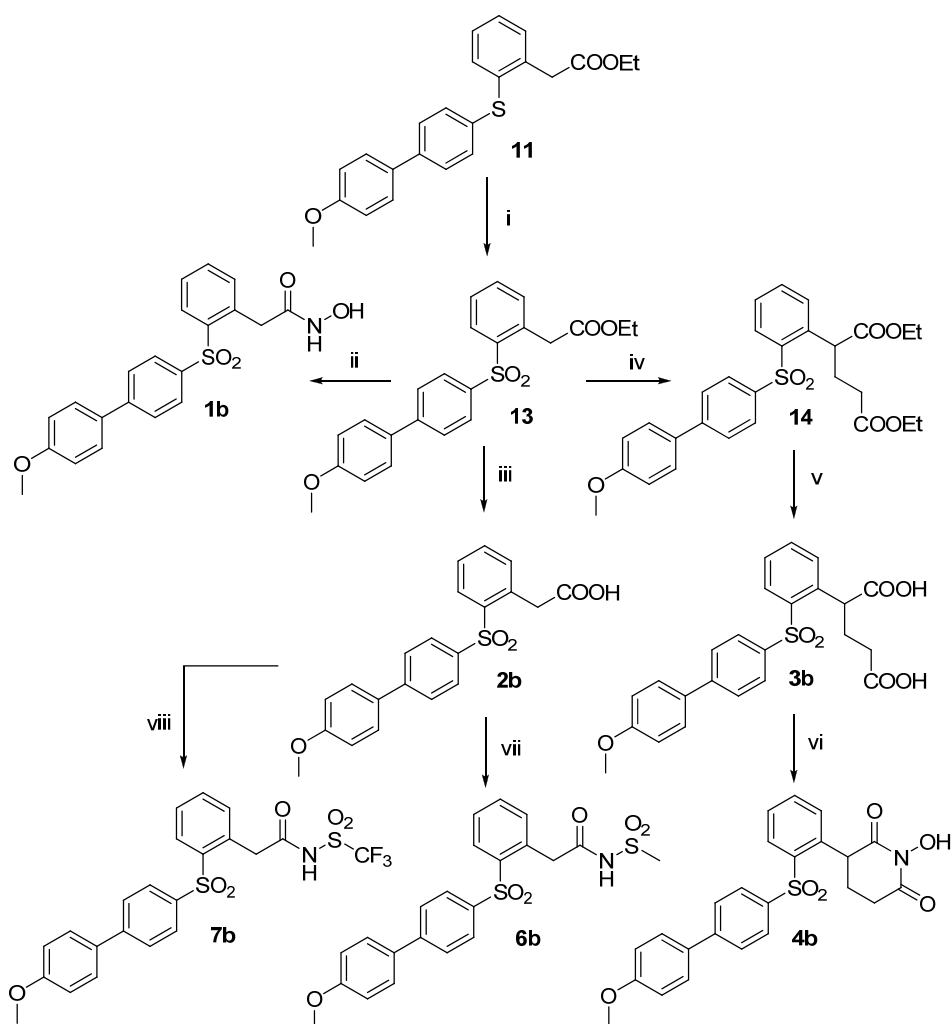
**Scheme 2.** Synthesis of compounds **3a** and **4a**. Reagents and conditions: i) ethyl acrylate, NaH, *t*BuOH/DMF, 4 h, 58%; ii) KOH, H<sub>2</sub>O, 130 °C, 16 h, 88%; iii) ethyl chloroformate, NMM, NH<sub>2</sub>OH·HCl, KOH, THF/MeOH, 4 h, 40%.

A similar sequence of reactions was followed to synthesize the diarylsulfone derivatives **1-4b**, **6b** and **7b** as detailed in Scheme 3. The hydroxamate **1b** and carboxylate **2b** were prepared following a route different from the one previously described,<sup>12</sup> which gave improved yields. The ethyl ester **11** was oxidized to the corresponding sulfone **13**, using potassium peroxymonosulfate (Oxone) in a solution of THF/MeOH/H<sub>2</sub>O. Subsequently, the ethyl ester **13** was hydrolyzed (NaOH 1N/dioxane) to the carboxylic acid **2b** which was transformed into the corresponding *N*-acylmethanesulfonamide **6b** and *N*-acyl(trifluoromethane)sulfonamide **6b** as described above for compounds **6a** and **7a** (Scheme 1). The ethyl ester **13** was also converted into the diethyl ester **14** through a Michael addition, using similar conditions to those previously described for diester **12** (Scheme 2). The diethyl ester **14** was hydrolyzed (KOH/H<sub>2</sub>O), to give the dicarboxylic acid **3b**. The last compound was firstly transformed into an *O*-benzylic cyclic intermediate by reaction with *O*-benzylhydroxylamine hydrochloride in the presence of triethylamine (TEA), EDC and 1-hydroxybenzotriazole (HOBT).<sup>20</sup> Then, the *O*-benzyl protecting group was removed by treatment with boron trichloride (BCl<sub>3</sub>) in controlled conditions (30 min at 0 °C

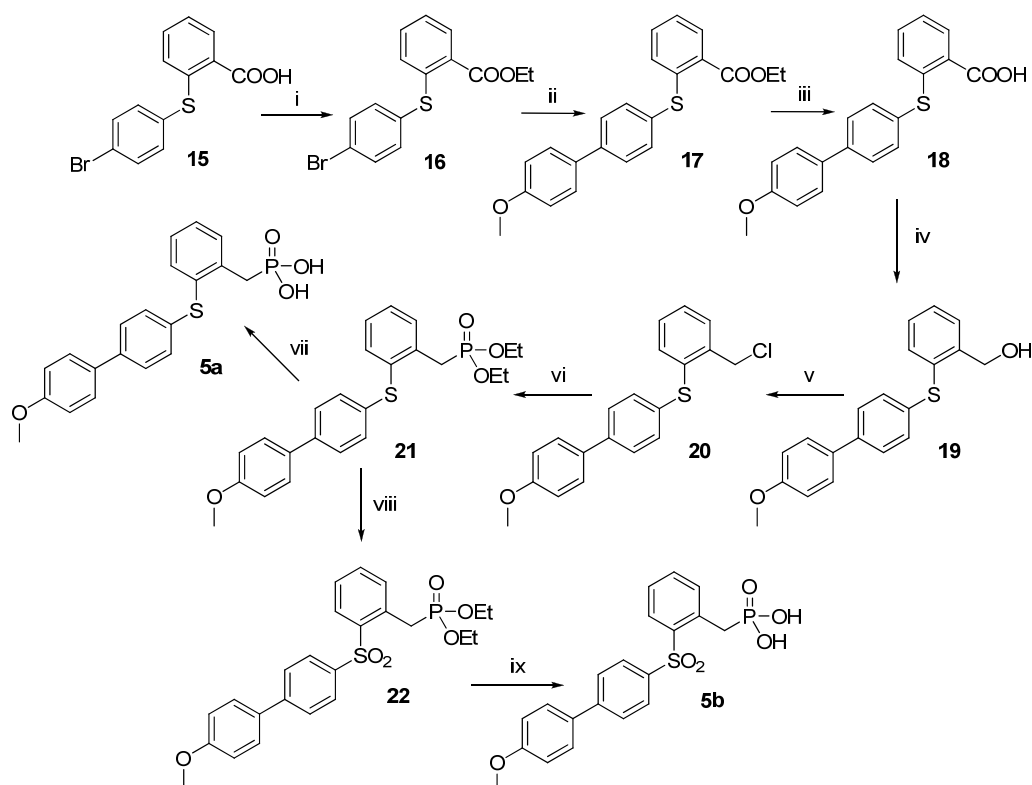


under nitrogen atmosphere) to give the *N*-hydroxypiperidin-dione **4b**. Finally, hydroxamic acid **1b** was obtained directly from ethyl ester **13** by reaction with hydroxylamine hydrochloride and KOH in a mixture of methanol/dioxane.

The synthesis of phosphonic acids **5a** and **5b** is described in the Scheme 4. The known 2-(4-bromophenylthio)benzoic acid **15**,<sup>12</sup> was protected as ethyl ester **16** and submitted to a palladium-catalysed cross-coupling (Suzuki conditions) with 4-methoxyphenylboronic acid to afford biphenyl derivative **17**. A basic hydrolysis of **17** with NaOH 1N in dioxane provided the carboxylic acid **18**, which was reduced with borane-tetrahydrofuran (BH<sub>3</sub>-THF 1M) to give benzylic alcohol **19**. The chloride derivative **20**, obtained by treatment of **19** with SOCl<sub>2</sub> in CH<sub>2</sub>Cl<sub>2</sub>, was transformed into the phosphonate derivative **21** by direct reaction with triethyl phosphite (P(OEt)<sub>3</sub>) at 130 °C (Arbuzov reaction). The phosphonic ester **21** was deprotected using trimethylsilyl bromide (TMSBr) in acetonitrile at 0 °C to give the phosphonic acid **5a**. Moreover, the oxidation of **21** with Oxone afforded the corresponding sulfone derivative **22** which, after acid hydrolysis with HCl 12N under reflux, gave the sulfone phosphonic acid **5b**.

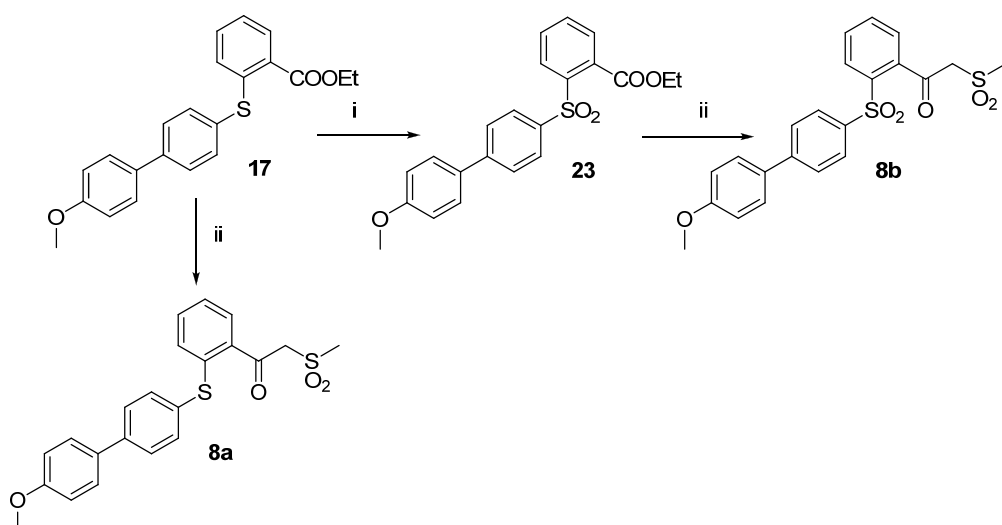


**Scheme 3.** Synthesis of compounds **1-4b** and **6b**, **7b**. Reagents and conditions: i) Oxone, THF/MeOH, H<sub>2</sub>O, 48 h, quant.; ii) NH<sub>2</sub>OH HCl, KOH, MeOH, 16 h, 50%; iii) NaOH 1N, dioxane, 16 h, 93%; iv) ethyl acrylate, NaH, *t*BuOH/DMF, 4 h, 97%; v) KOH, H<sub>2</sub>O, 130 °C, 16 h, 68%; vi) (1) NH<sub>2</sub>OBn HCl, TEA, EDC, HOBT, CH<sub>2</sub>Cl<sub>2</sub>, 72 h, 51%; (2) BCl<sub>3</sub>, CH<sub>2</sub>Cl<sub>2</sub>, 0 °C, 1 h, 73%; vii) CH<sub>3</sub>SO<sub>2</sub>NH<sub>2</sub>, EDC, DMAP, CH<sub>2</sub>Cl<sub>2</sub>, 5 h, 56%; viii) CF<sub>3</sub>SO<sub>2</sub>NH<sub>2</sub>, EDC, DMAP, CH<sub>2</sub>Cl<sub>2</sub>, 5 h, 81%.



**Scheme 4.** Synthesis of compounds **5a** and **5b**. Reagents and conditions: i) EDC, DMAP, EtOH, CH<sub>2</sub>Cl<sub>2</sub>, RT, 18h, 82%; ii) 4-methoxyphenylboronic acid, Pd(PPh<sub>3</sub>)<sub>4</sub>, Na<sub>2</sub>CO<sub>3</sub>, toluene/EtOH, 100 °C, 5 h, 87%; iii) NaOH 1N, dioxane, RT, 48 h, quant.; iv) BH<sub>3</sub> THF 1M, RT, 26 h, 33%; v) SOCl<sub>2</sub>, CH<sub>2</sub>Cl<sub>2</sub>, RT, 1 h, 82%; vi) P(OEt)<sub>3</sub>, 130 °C, 6h, 53%; vii) TMSBr, MeCN, 0°C to RT, 12 h, 69%; viii) Oxone, THF/MeOH, H<sub>2</sub>O, RT, 16h, 89%; ix) HCl 12N, reflux, 20 h, 60%.

Methylsulfonyl ethanone derivatives **8a,b** were synthesized as reported in Scheme 5. Ethyl ester **17** was oxidized by treatment with Oxone to the corresponding sulfone **23**. Both esters **17** and **23** were respectively converted into final compounds **8a** and **8b** by reaction with dimethyl sulfone and potassium *tert*-butoxide in DMSO.



**Scheme 5.** Synthesis of compounds **8a** and **8b**. Reagents and conditions: i) Oxone, THF/MeOH, H<sub>2</sub>O, RT, 48 h, 78%; ii) dimethyl sulfone, *t*-BuOK, DMSO, 60 °C, 1.5 h, 18-20%.

### 2.3. MMPs Inhibition.

The newly synthesized compounds **1-8a** and **3-8b** were tested on human recombinant MMP-12 by fluorometric assay to evaluate their inhibitory activity *in vitro*, in comparison with the previously reported sulfones **1b** and **2b**. Initially their selectivity over the other members of the MMP family was examined by testing them on MMP-2 and MMP-9 (gelatinases), two important proteolytic enzymes respectively involved in cancer and vascular pathologies. Gelatinases differ from MMP-12 by having an “intermediate S1’ pocket”, whereas the latter is classified as a “deep S1’ pocket MMP”.<sup>21</sup> Improved selectivity for MMP-12 over gelatinases could be indicative of the ability of the new compounds to discriminate among the various MMP family members. However, a recent study<sup>22</sup> conducted on a common COPD animal model, using long-term cigarette smoke (CS) exposed mice, showed changes in the expression levels of MMPs in the lungs confirmed by western blot analysis. Expression of both MMP-12 and MMP-9 were significantly increased in the CS group. Therefore they concluded that while MMP-12 is an essential mediator of the pathophysiology of COPD, MMP-9 can be considered as an indicator of the clinical COPD stage.

Inhibitory activity data are reported in Table 1. In general, diaryl sulfide derivatives possessed a higher affinity for MMP-12 than the corresponding sulfones. Moreover, in accordance with previously reported data, both activity and selectivity for this class of compounds with a common backbone depend on which ZBG is used. As expected, hydroxamate derivatives possessed the highest activity ( $IC_{50} = 4$  nM on MMP-12) in both series of compounds but a poor selectivity over the other MMPs tested. The best results in terms of activity and selectivity for MMP-12 were obtained with *N*-1-hydroxypiperidine-2,6-dione derivatives **4a,b**, and in particular with sulfide **4a** which presented an  $IC_{50} = 33$  nM on MMP-12 with a 176-fold selectivity over MMP-9 and 20-fold selectivity over MMP-2. Diaryl sulfide **3a** bearing a dicarboxylic acid as ZBG displayed a similar activity, with an  $IC_{50} = 26$  nM on MMP-12 and a good selectivity over MMP-9 and MMP-2. All derivatives of both series (S and SO<sub>2</sub>) with “soft-binders” as the ZBG (**6-8a,b**) showed reduced activity on all the MMPs tested ( $IC_{50} > 3$   $\mu$ M) and the methylsulfonyl ethanone derivatives **8a,b** were totally inactive ( $IC_{50} > 100$   $\mu$ M). Phosphonate (**5a,b**) and carboxylate (**2a,b**) derivatives showed a moderate activity ( $40 < IC_{50} < 600$  nM) towards MMP-12 with sulfide compounds endowed with a higher potency than sulfone analogues.

**Table 1.** *In vitro*<sup>a</sup> inhibitory activity ( $IC_{50}$ , nM) of diaryl sulfides **1-8a** and diaryl sulfones **1-8b** on MMPs.

Compd	MMP-2	MMP-9	MMP-12
<b>1a</b>	6.8	120	4.0
<b>1b</b>	9.7	94	4.8
<b>2a</b>	114	830	40
<b>2b</b>	47	730	140
<b>3a</b>	660	2960	26
<b>3b</b>	1350	14300	510
<b>4a</b>	670	5800	33
<b>4b</b>	414	1430	40

<b>5a</b>	250	1120	250
<b>5b</b>	380	2500	600
<b>6a</b>	5300	18000	3300
<b>6b</b>	3600	3700	3500
<b>7a</b>	46000	50000	2100
<b>7b</b>	2500	24500	7500
<b>8a</b>	230000	332000	230000
<b>8b</b>	>10000	>10000	>10000

<sup>a</sup>Enzymatic data are mean values for three independent experiments performed in duplicate. SD were generally within  $\pm 10\%$ .

At this point, to better characterize the selectivity profile of the new HPD derivatives **4a,b** with respect to the corresponding hydroxamates **1a,b**, their activity was tested also on MMP-1 and MMP-14 (Table 2). The selectivity over these two MMPs is particularly important because their inhibition is considered responsible for the musculoskeletal side effects observed with broad-spectrum MMPI in clinical trials.<sup>23</sup>

**Table 2.** Selectivity profile of *N*-1-hydroxypiperidine-2,6-diones **4a** and **4b** in comparison with hydroxamates **1a** and **1b**.

Compd	IC <sub>50</sub> <sup>a</sup> (nM)				
	MMP-1	MMP-2	MMP-9	MMP-12	MMP-14
<b>4a</b>	260000	670	5800	33	40000
<b>4b</b>	>10000	414	1430	40	4000
<b>1a</b>	250000	6.8	120	4.0	2000
<b>1b</b>	8300	9.7	94	4.8	710

“The IC<sub>50</sub> values are the average of three determinations with a standard deviation of <10%.

HPD derivatives **4a,b** showed a higher selectivity for MMP-12 over MMP-14 with respect to the corresponding hydroxamates **1a,b**. The activity towards MMP-1, already poor for hydroxamates, was not affected by the change of ZBG. Moreover, in both classes of compounds, sulfide derivatives presented a better selectivity than sulfones.

These data suggest that the combined effects of sulfur oxidation state and the nature of the ZBG can determine the selectivity profile of the tested compounds. In fact, the combination of a sulfide group in the diaryl moiety and a *N*-1-hydroxypiperidine-2,6-dione as new ZBG, led to the identification of a derivative, **4a**, with a greatly improved selectivity for MMP-12 with respect to the hit compound **1b**.

#### **2.4. Solution equilibrium studies.**

Since the biological role of MMP inhibitors is largely determined by their interaction with Zn<sup>2+</sup> that is present at the enzyme active site, the chelating ability of the developed compounds towards this metal ion was evaluated through solution studies. These studies were conducted to determine the stability constants of the corresponding metal complexes and to establish the coordination modes of the corresponding metal complexes, as well as their speciation at different pH. For that purpose, twelve compounds – **1-4 (a,b)** and **6-7 (a,b)** – were studied through potentiometric titrations and nuclear magnetic resonance of proton spectroscopy (<sup>1</sup>H NMR). Compound **1b** was not studied since it was completely hydrolyzed to compound **2b**, at the chosen working medium, while the phosphonic derivatives **5a,b** were not considered herein since metal phosphonates are already well studied in the literature and stability constant values are expected to be similar to the ones already obtained for phosphoric acid ( $\log \beta_{ZnHL} = 14.14$ ).<sup>24</sup>

##### **2.4.1 Acid-base properties**

All the ligands, except **2a**, **7a** e **7b** ( $L^-$ ) or **3b** ( $HL^-$ ), were obtained in the neutral form, respectively  $H_2L$  (**3a**) and  $HL$  (**1a**, **2b**, **4a,b**, **6a,b**). Due to poor water solubility of some ligands, especially **1a** and **4a**, a mixed DMSO/water (60% w/w) medium was used in these studies. In fact, DMSO is a quite common and well tolerated solvent used in biological and cellular studies (with  $C_{\text{ligand}} < 7 \mu\text{M}$ ), and so the herein used medium would correspond to a quite low DMSO concentration ( $< 1\%$ ) with concomitant no alterations in tissues.<sup>25</sup>

A brief analysis of the protonation constants (Table 1S, Supporting Information) allows to conclude that the sulfide and sulfonyl groups have negligible effect on  $\log K$ , because they are too far from the labile protons. The  $\log K$  values for the cyclic HPD derivatives **4a,b** (9.03-9.35) are lower than for the simple hydroxamate derivative **1a** (10.29), due to electron delocalization (resonance and inductive effects due to the extra carbonyl group). Regarding the sulfonamide derivatives, the protonation constants drop drastically - **6a,b** ( $\log K \sim 5.5$ ) and **7a,b** ( $\log K < 2$ ) - due to electron withdrawing effect of trifluoromethyl group.

The profiles of the species distribution curves (Figure 1S, Supporting Information) show that under physiological conditions (pH 7.4) the predominant species is  $L^-$  or  $L^{2-}$  for all the compounds, except for the hydroxamate derivatives (**1a**, **4a** and **4b**) for which only the neutral  $HL$  species is present. The predominance of anionic species at physiological conditions may be expected to convey some hydrophilic character.

#### 2.4.2. Studies on Zn(II) complexation

The chelating ability of the compounds towards Zn(II) was evaluated by determining the global formation constants of the complexes, by pH-potentiometric titrations at 1:1 and 1:2 metal-to-ligand molar ratios, and curve fitting with Hyperquad 2008 program. Analysis of the titration curves showed a drop in the deprotonation profile of the ligand curve due to the presence of the metal ion, such as in Figure 2 for ligand **7a**) and  $0 < a < 1$ , therefore evidencing the formation of metal complexes. Fitting



analysis of the overall potentiometric titration data shows that the Zn(II) complex formation occurs predominantly for pH between 3 and 8, with the presence mainly of 1:1 and 1:2 Zn/L species for all the compounds except **2a**, **6a** and **7a,b**, for which 1:2 species were not found (Table 1S, Figure 3 and Figure 2S, Supporting Information).

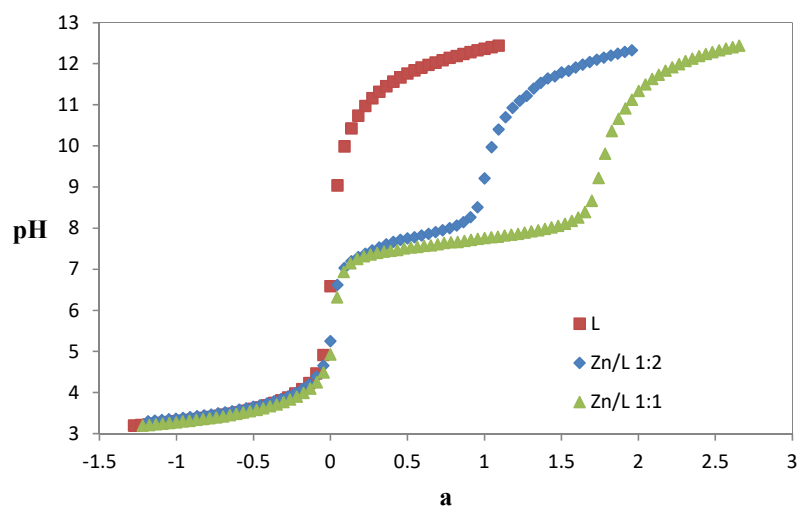


**Figure 2.** Potentiometric titration curves for **7a** alone and in the presence of  $\text{Zn}^{2+}$  at 1:1 and 1:2 metal-to-ligand molar ratios ( $C_L = 6.7 \times 10^{-4}$  M in 60% w/w DMSO/water).

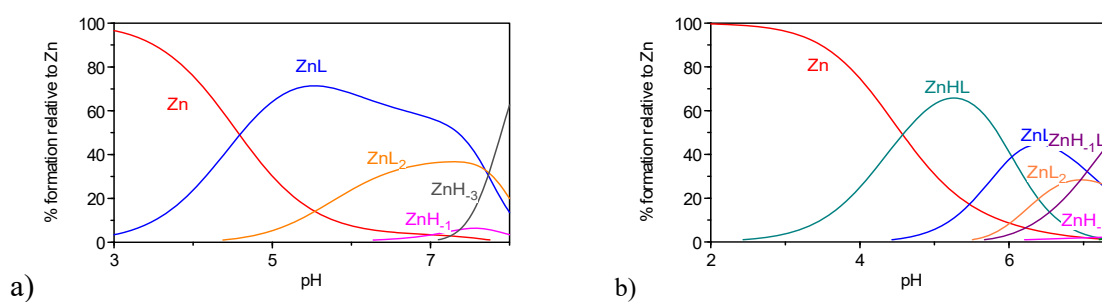


**Figure 3.** Species distribution curves of two ligand- $\text{Zn}^{2+}$  systems at 1:2 metal-to-ligand molar ratios (Zn:L): a) **2b**, b) **3b** ( $C_L = 6.7 \times 10^{-4}$  M in 60% w/w DMSO/water).

Aimed to get some insight on the coordinating groups for each compound,  $^1\text{H}$  NMR spectra were performed for compounds (**L**) as well as for the respective 1:1 and 1:2 Zn/L systems. The results obtained for **1a** (Figure 3Sa, Supporting Information) and **4a,b** predict a (*O,O*)-hydroxamate coordination mode, as found for acetohydroxamic acid (AHA) in  $\text{M}(\text{AHA})_2$ <sup>26</sup> and for *N*-benzyl-*N'*-hydroxypiperazine-2,6-dione (BHPD) in  $\text{M}(\text{BHPD})_2$ .<sup>27</sup> Regarding the sulfonamides (**6a,b** and **7a,b**) mainly 1:1 ZnL complexes are formed, involving a *N,O* or most probably a *N,O,O* coordination to the metal ion, namely with the amidine nitrogen and a carbonyl and a sulfonyl oxygen in the 6-member ring metal coordination mode.

Comparison of the zinc binding affinity of the compounds was based on the pZn values (pH = 6, to avoid metal hydrolysis) instead of the global stability constants, due to differences in equilibrium models and acid-base properties. The pZn value is usually defined as the negative logarithm of the concentration of the free metal ion in solution, for total concentration of metal 1  $\mu\text{M}$  and 10-fold excess of ligand, at physiological pH 7.4, but it can be used under other pH conditions.<sup>28</sup>

**Table 3.** pZn<sup>a</sup> values obtained for the compounds ( $T = 25.0 \pm 0.1$  °C,  $I = 0.1$  M KCl, 60% w/w DMSO/water).

Comp.	1a	2a	2b	3a	3b	4a	4b	6a	6b	7a	7b
pH											
6.0	6.04	6.04	6.1	6.04	6.14	6.05	6.13	6.10	6.56	6.75	6.91

<sup>a</sup> pZn =  $-\log[\text{Zn}(\text{II})]$  with  $C_L/C_{\text{Zn}} = 10$  and  $C_{\text{Zn}} = 10^{-6}$  M

The obtained pZn values are quite similar (pZn ~ 6), but a more detailed analysis of the data evidenced some differences (Table 3). For the stoichiometric conditions used in this study, the introduction of the second carboxylic group (compare **2a**, **3a** and **2b**, **3b**) does not improve the stability of the zinc

complexes, because the size of its ethylene linker is too long to allow bischelating coordination (7-member ring). Regarding the sulfonamide derivatives, **6a,b** and **7a,b**, the respective pZn values (6.1-6.9) suggest an increase of complex stability for trifluoromethyl derivatives.

Overall, based on equilibrium solution and <sup>1</sup>H NMR studies for the zinc complexation with this set of ligands, equilibrium models and respective coordination modes were proposed, allowing a comparative analysis of their relative affinity for zinc. In spite of the diversity of functional groups, the pZn values appear quite similar (pZn ~ 6), except for the trifluoromethane sulfonamide derivatives (pZn ~ 7). However, it must be stated that the inhibitory capacity of the compounds does not depend only on the zinc chelating capacity of their binding group, measured in solution, but hangs on many factors, such as the conformation of the inhibitor and its accommodation and interactions within the enzyme active site and subsites.

## 2.5. Crystallographic studies.

The crystal structures for inhibitors **1b**, **2b**, **3a,b** (Figure 4) were obtained in three different polymorphs with 1-4 molecules in the asymmetric unit in complex with MMP-12 and for **3a** in complex with MMP-9 (Supporting Information, Table 3S). The packing is different between the two polymorphs in space groups P2<sub>1</sub>2<sub>1</sub>2<sub>1</sub> and C2 (respectively, PDB codes: 6ENM and 6EDX), although the protein construct is the same. In the 6EDX structure, grown in space group C2, which diffracts to 1.3 Å resolution, the N-terminal residues from Gly106 onwards are visible. But, for the P2<sub>1</sub>2<sub>1</sub>2<sub>1</sub> polymorph, which diffracts to lower resolution (1.59 Å, 6ENM), the N-terminal density is visible only from His112 onwards. In the C2 polymorph, this six-residue segment from Gly106 to Lys111 is well-ordered and packs against the loops and turns between Pro187 and Tyr262, while in the P2<sub>1</sub>2<sub>1</sub>2<sub>1</sub> polymorph crystal contacts between monomers A and B occupy the same zone. Nonetheless, the differences in crystal packing between these two polymorphs are far from the zinc sites and do not alter significantly the modes of ligand binding. All the crystals diffract to near atomic resolution, from 1.6 Å

to 1.1 Å, as defined by Diederichs et al.<sup>29</sup>. The Fo-Fc Fourier maps contoured at 3 $\sigma$  reveal the ligand positions in the electron density for all the structures (Figure 4) and no significant changes can be detected regarding the protein conformation. The 2Fo-Fc Fourier maps contoured at 1 $\sigma$  are also shown in Figure 4S, Supporting Information. Even if the Fo-Fc density at 3 $\sigma$  is not complete for compound **2b**, our attempts to fit the ligand into other binding modes did not reveal suitable 2Fo-Fc density, and in each case strong Fo-Fc density appeared in the S1' pocket. Thus the presence of compound **2b** in the S1' binding site is confirmed, even though its LLDF<sup>30</sup> value of 3.31 is slightly higher than the recommended threshold value 2.0. However, recent discussions point out the unreliability of LLDF as a metric<sup>31</sup> and, in our experience, even LLDF values as high as 5, do not exclude the presence of the ligand.

HPD derivatives **4a** and **4b** did not crystallize in complex with the MMP-12 catalytic domain at a pH under which these two compounds are stable. The only crystal structures obtained with **4a** and **4b**, at high pH (9.5-10),<sup>14</sup> showed degraded ligands.

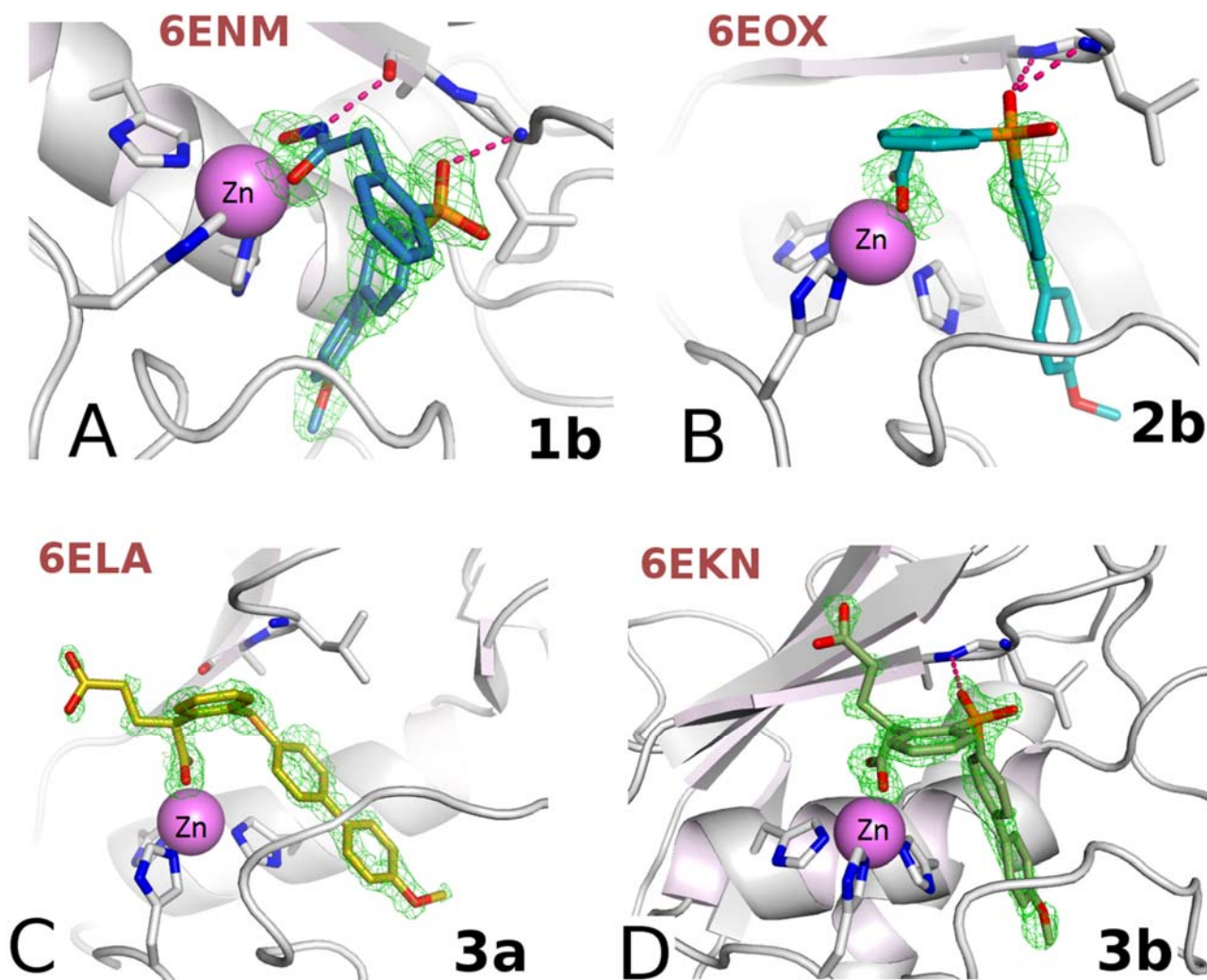


**Figure 4. Fo-Fc maps contoured at  $3\sigma$  for the inhibitors in complex with MMP-12.** The PDB codes for the structures are shown in red. (A) The electron density for the hydroxamic inhibitor **1b** (PDB ID: 6ENM). (B) The electron density for the carboxylic analog **2b** (PDB ID: 6EOX) is much weaker than for **1b** coherent with an LLDF<sup>30</sup> = 3.13. (C) The electron density for inhibitors **3a** (PDB ID: 6ELA) and (D) **3b** are similar (PDB ID: 6EKN). All the inhibitors, in both structures have negative LLDF values.

All of the inhibitors with a sulfonyl functional group superimpose well on each other (Figure 5A), although for the inhibitor **3b** the phenyl ring is slightly moved probably in order to place the ethylene-carboxylate chain (a chain of the pentanedioic acid group, where the other carboxylate is the ZBG). A small shift in the position of the sulfonyl group is dictated by the change of the ZBG from a carboxylic

to a hydroxamic chelator (Figure 5B). The superposition between **1b** and **3b** also displays slightly a different orientation of the phenyl group in the hydroxamic derivative.

The comparison between the sulfonyl and sulfide derivatives (**3b** and **3a**, Figure 5C) shows that despite the fact that the biphenyls sit in the S1' pocket and that the chelating groups are unmoved, the sulfonyl linker slightly re-orientates the phenyl moiety and the position of the ethylene-carboxylate chain. The sulfonyl linker forms two extra strong H-bonds with the amide nitrogen of Leu181 and the amide nitrogen of Ala182 of the MMP-12 backbone. As a consequence, the biphenyl group is partially displaced out of the S1' pocket, and the phenyl moiety is re-orientated so that the ethylene-carboxylate group interacts differently with the sidechain of His183 (Figure 5G). For the sulfide derivative this interaction is mediated by a water molecule (Figure 5E), while for the sulfonyl derivative a direct H-bond is made to ND1 of His183. These differences in binding may explain the reduction in potency of the sulfonyl derivatives (**3b**) compared to the sulfide derivatives (**3a**).

The binding mode of the sulfide derivative **3a** appears to be common to both MMP-12 and MMP-9 (Figure 5D). The almost perfect superposition of the inhibitor on the two enzymes makes it difficult to understand which elements might determine the selectivity. In the top portion of the binding site, one residue distinguishes MMP-12 from MMP-9: at MMP-12 position 180, an Ile residue is present, while at the equivalent position there is a Leu in MMP-9. The Ile in the MMP-12-**3a** complex (PDB: 6ELA) is clearly defined by a single conformation while the same residue in the MMP-12-**3b** crystal structure (PDB: 6EKN) is found in two alternative conformations. A double conformation for the equivalent Leu residue is also observed in MMP-9 (PDB: 6ESM). However, the most likely contribution to the selectivity between MMP-12 and MMP-9 may lie elsewhere. The root mean square derivation (RMSD) calculated on C $\alpha$  of the 152 residues between monomer A of MMP-9 and the four chains of MMP-12 gave very similar values ranging from 0.65 Å to 0.75 Å. The comparison between the binding of **3a** to MMP-9 and MMP-12 shows also a difference in positioning of the ligand within the S1' pocket, with a

RMSD value of 0.90 Å between the two ligands (Figure 5D). The most striking difference between the structures of the two enzymes lies at Arg249 in MMP-9, which forms a direct H-bond to an opposing main chain carbonyl oxygen of Glu241 (3.2 Å), in the S1' pocket. In MMP-12, the corresponding residues are Ala241 and Lys233, respectively (Figure 5S, Supporting Information), and the Ala241 side chain cannot form a direct H-bond to the carbonyl of Lys233. Other more subtle differences occur in the stretch of residues between Glu241 and Pro255 (MMP-9), which wraps around the biphenyl moieties of the ligand and where there are a number of sequence variations (Figure 5S). In the tertiary coordination sphere of the ligand **3a**, there is an insertion of one residue in the MMP-9 segment between Leu209 and Tyr218, which shifts the loop relative to MMP-12 (Figure 5S). Even though the S1' pockets are rather similar between the two enzymes, it is expected that their subtle differences in sequence and position are likely to give a major contribution to selectivity. Not only is the positioning of **3a** almost identical in MMP-9 and MMP-12, but also the water molecule that mediates the interaction between the **3a** carboxylate and His 183 (MMP-12 numbering) is strictly conserved (Figure 5E). Given the high resolution of the structures, in particular for MMP-9 where the individual atoms are clearly defined (Figure 5F), the accuracy in the ligand positioning is irrefutable.

As a result of the different interactions established by the sulfide and sulfonyl derivatives, the two classes of MMP inhibitors should be treated separately. Comparison of sulfonyl derivatives bound to MMP-12 and MMP-9 (for example 4H82, 5I12 or 4H3X)<sup>32</sup> shows that the binding mode of these derivatives is conserved. The best superposition between ligands in all these structures is obtained at the biphenyl moiety rather than at the sulfonyl position, coherent with the role of the ZBG that can alter the sulfonyl position.

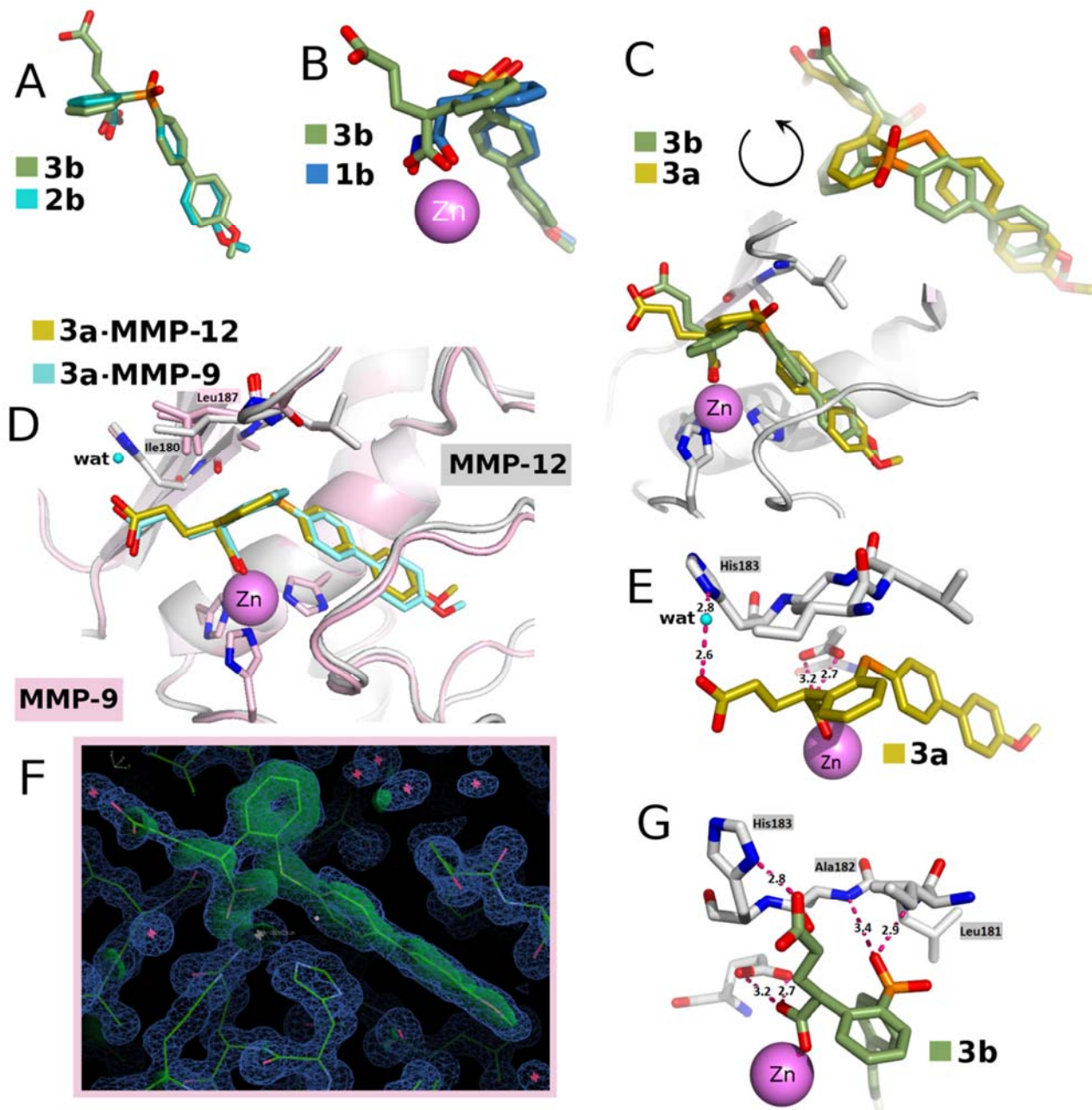


**Figure 5. Comparison of ligand binding.** The H-bonds are displayed as red dashed lines. (A) Superposition of inhibitors **2b** and **3b** bound to MMP-12. (B) Superposition of inhibitors **1b** and **3b** bound to MMP-12. (C) Superposition of inhibitors **3a** and **3b** bound to MMP-12. (D) Comparison of the binding of **3a** (MMP-12: gold; MMP-9: cyan) to MMP-12 (gray) and MMP-9 (rose). RMSD value is 0.90 Å between the atoms of the two ligands. (E) H-bonded interactions between **3a** and MMP-12. (F) 3D surface representation of the MMP-12 active site with **3a** in green. (G) H-bonded interactions between **3b** and MMP-12.



(F) Electron density from COOT<sup>33</sup> showing individual atoms around the MMP-9 catalytic zinc for the complex with **3a** to highlight the high resolution obtained from the trigonal polymorph of MMP-9. The Fo-Fc Fourier map is contoured at 3  $\sigma$  in green and the 2Fo-Fc Fourier map is contoured at 1  $\sigma$  in blue mesh. (G) H-bonded interactions between **3b** and MMP-12.

### 3. Conclusions

In the present study, a new series of thioaryl-based MMP-12 inhibitors bearing alternative ZBGs was developed and evaluated. Starting from the promising results previously obtained with two 4-methoxybiphenylsulfonyl hydroxamate and carboxylate-based (**1b** and **2b**) inhibitors, we modified the nature of the ZBG and the sulfur oxidation state with the aim of improving the selectivity for MMP-12. The new compounds were tested on human MMPs by using a fluorometric assay. In general, diaryl sulfide derivatives possessed a higher affinity for MMP-12 than the corresponding sulfones. In particular, the best results in terms of activity and selectivity for MMP-12 were obtained with sulfide **4a**, presenting a *N*-1-hydroxypiperidine-2,6-dione (HPD) group as new ZBG. This cyclic hydroxamate showed an IC<sub>50</sub> = 33 nM on MMP-12 with a 1200-fold selectivity over MMP-14, 176-fold selectivity over MMP-9 and 20-fold selectivity over MMP-2, thus resulting more selective than the starting hydroxamate **1b**. Diaryl sulfide **3a**, bearing a dicarboxylic acid as ZBG, displayed a similar activity, with an IC<sub>50</sub> = 26 nM on MMP-12 and a good selectivity over MMP-9 and MMP-2. Solution complexation studies with Zn<sup>2+</sup> were performed to characterize the chelating abilities of the new compounds. HPD derivatives **4a,b** were confirmed to be bidentate and quite strong Zn(II) chelators, comparable to the non-cyclic hydroxamate **1a**, while **3a** coordinates as a monocarboxylic ligand. Moreover, X-ray crystallographic studies performed on the complexes of **3a** and **3b** with MMP-12 and **3a** with MMP-9 clarified the binding mode in the catalytic domain, but did not fully elucidate the reasons for the selectivity of these new dicarboxylic derivatives.

This preliminary study allowed us to identify a hit compound with a new ZBG endowed with a good selectivity for MMP-12. Further optimization efforts are ongoing with the aim of improving the hydrophilicity and bioavailability of the new HPD sulfide **4a** before testing it in cell-based and *in vivo* models of cardiovascular or pulmonary pathologies.

#### 4. Experimental section.

**4.1. Chemistry.** Melting points were determined on a Kofler hotstage apparatus and are uncorrected. <sup>1</sup>H, <sup>13</sup>C and <sup>19</sup>F NMR spectra were determined with a Varian Gemini 200 MHz spectrometer or a Bruker Avance III HD 400 MHz spectrometer. Chemical shifts ( $\delta$ ) are reported in parts per million and coupling constants (*J*) are given in hertz (Hz). The following abbreviations are used: singlet (s), doublet (d), triplet (t), double-doublet (dd), double-triplet (dt), broad (br) and multiplet (m). Chromatographic separations were performed on silica gel columns by flash column chromatography (Kieselgel 40, 0.040–0.063 mm; Merck) or using Isolute Flash Si II cartridge (Biotage). Reactions were followed by thin-layer chromatography (TLC) on Merck aluminum silica gel (60 F254) sheets that were visualized under a UV lamp and hydroxamic acids were visualized with FeCl<sub>3</sub> aqueous solution. Evaporation was performed *in vacuo* (rotating evaporator). Sodium sulfate was always used as the drying agent. Commercially available chemicals were purchased from Sigma-Aldrich (Milan, Italy). Elemental analysis has been used to determine purity of the described compounds, which is >95%. Analytical results are within  $\pm 0.40\%$  of the theoretical values (Table 2S in Supporting Information).

**2-(2-((4'-Methoxy-[1,1'-biphenyl]-4-yl)thio)phenyl)acetic hydroxamic acid (1a).** To a solution of *N*-hydroxylamine hydrochloride (1.882 g, 27.08 mmol) in MeOH (13.21 mL), powdered KOH (1.518 g, 27.08 mmol) was added portionwise at 0 °C. After the addition, the solution was stirred for 1h at RT. The precipitate of KCl was filtered off and the filtrate containing the appropriate free hydroxylamine was added dropwise to an ice cooled solution of the ethyl ester **11** (50 mg, 0.132 mmol) dissolved in

MeOH (2 mL). Subsequently, an additional amount of powered KOH was added (until pH = 9) and the reaction was stirred at RT overnight. The solvent was evaporated in vacuo, the residue was treated with a saturated solution of NH<sub>4</sub>Cl and extracted with EtOAc (3 x 25mL). The combined organic phases were washed with brine, dried over Na<sub>2</sub>SO<sub>4</sub>, filtered and evaporated under reduced pressure. Compound **1a** was obtained without further purification as a white powder (42 mg; 88% yield). M.p. 160-162 °C. <sup>1</sup>H NMR (400 MHz, DMSO-*d*<sub>6</sub>) δ: 3.55 (s, 2H); 3.79 (s, 3H); 7.00-7.03 (m, AB system, 2H); 7.22-7.42 (m, Ar, 6H); 7.58-7.63 (m, Ar, 4H); 8.85 (s, 1H); 10.64 (s, 1H). <sup>13</sup>C NMR (100 MHz DMSO-*d*<sub>6</sub>) δ: 37.28; 55.18; 114.41; 127.09; 127.63; 127.91; 128.05; 130.23; 130.83; 131.55; 133.08; 134.06; 137.61; 138.36; 159.03; 166.14; 166.55.

**2-(2-((4'-Methoxy-[1,1'-biphenyl]-4-yl)sulfonyl)phenyl)acetic hydroxamic acid (1b)**<sup>12</sup>. The title compound was synthesized as previously reported for the preparation of compound **1a**, starting from ethyl ester **13** (100 mg, 0.2436 mmol). The product was purified by a trituration in Et<sub>2</sub>O collecting 48 mg of compound **1b** (50% yield). M.p. 158 °C. <sup>1</sup>H NMR (400 MHz, DMSO-*d*<sub>6</sub>) δ: 3.81 (s, 3H); 3.94 (s, 2H); 7.05-7.07 (m, AB system, 2H); 7.44-7.46 (m, Ar, 1H); 7.56-7.70 (m, Ar, 4H); 7.84-7.96 (m, Ar, 4H); 8.10-8.12 (m, Ar, 1H); 8.87 (s, 1H); 10.62 (s, 1H). <sup>13</sup>C NMR (100 MHz, DMSO-*d*<sub>6</sub>) δ: 31.16; 55.74; 115.06; 127.51; 128.28; 128.55; 128.91; 129.75; 130.80; 134.19; 134.64; 139.33; 139.40; 145.16; 160.38; 171.94.

**2-(2-((4'-Methoxy-[1,1'-biphenyl]-4-yl)thio)phenyl)acetic acid (2a)**. The ethyl ester **11** (500 mg, 1.321 mmol) was dissolved in a minimum amount of dioxane. Subsequently, 2 equiv. of NaOH 1N (2.7 mL) were added to the stirred solution. The reaction mixture was stirred at RT overnight. After the evaporation of dioxane, water was added and the mixture was acidified with HCl 1N until pH = 1. The white precipitate was filtrated off and washed with water. Compound **2a** was obtained as a white powder without any further purification (459 mg; quantitative yield). M.p. 185-187 °C. <sup>1</sup>H NMR (400 MHz, CD<sub>3</sub>OD) δ: 3.79 (s, 2H); 3.82 (s, 3H); 6.96-6.99 (m, AB system, 2H); 7.20-7.24 (m, Ar, 3H); 7.3

(dt,  $J_1=7.6$  Hz,  $J_2=1.4$  Hz, Ar, 1H); 7.35-7.39 (m, Ar, 2H); 7.48-7.54 (m, 2 AB system, 4H).  $^{13}\text{C}$  NMR (100 MHz, DMSO- $d_6$ )  $\delta$ : 40.81; 55.19; 114.41; 127.03; 127.64; 128.05; 129.95; 131.43; 131.62; 133.28; 133.86; 134.50; 138.13; 138.96; 159.00; 172.5.

**2-(2-((4'-Methoxy-[1,1'-biphenyl]-4-yl)sulfonyl)phenyl)acetic acid (2b)**<sup>12</sup>. The title compound was synthesized following the procedure described above for the preparation of compound **2a**, starting from ethyl ester **13** (130 mg, 0.316 mmol). After work-up, compound **2b** was obtained as a white powder without any further purification (92 mg; 93% yield). M.p. 189 °C.  $^1\text{H}$  NMR (400 MHz, DMSO- $d_6$ )  $\delta$ : 3.81 (s, 3H); 3.95 (s, 2H); 7.06-7.08 (m, AB system, 2H); 7.45 (dd, Ar,  $J_1=7.6$  Hz,  $J_2=1.2$  Hz, 1H); 7.59 (dt,  $J_1=1.4$  Hz,  $J_2=7.8$  Hz, Ar, 1H); 7.66-7.72 (m, Ar, 3H); 7.85-7.90 (m, Ar, 4H); 8.11 (dd,  $J_1=7.9$  Hz,  $J_2=1.3$  Hz, Ar, 1H); 12.34 (s, 1H).  $^{13}\text{C}$  NMR (100 MHz, DMSO- $d_6$ )  $\delta$ : 35.71; 55.23; 114.50; 126.91; 127.66; 127.90; 128.33; 129.17; 130.26; 132.85; 133.47; 134.94; 138.77; 138.93; 144.58; 159.78; 165.73.

**2-(2-((4'-methoxy-[1,1'-biphenyl]-4-yl)thio)phenyl)pentanedioic acid (3a)**. A mixture of diethyl ester **12** (219 mg, 0.486 mmol) and aqueous solution of KOH (272 mg, 4.861 mmol in 7.84 mL water) was stirred overnight at 130 °C. After being cooled to RT the reaction mixture was acidified with HCl 1N until pH strongly acidic. The resulting white precipitate was filtered off and washed with water. The crude product was purified by trituration with *n*-hexane/ $\text{CH}_2\text{Cl}_2$  1:1 to give the final compound **3a** as a white solid (180 mg, 88% yield). M.p. 190-193 °C.  $^1\text{H}$  NMR (400 MHz, DMSO- $d_6$ )  $\delta$ : 1.86-1.90 (m, 1H); 2.1-2.24 (m, 3H); 3.8 (s, 3H); 4.26 (t,  $J_1=7.3$  Hz, 1H); 7.00-7.03 (m, AB system, 2H); 7.28-7.39 (m, Ar, 6H); 7.58-7.61 (m, Ar, 4H); 12.27 (s, 2H).  $^{13}\text{C}$  NMR (100 MHz DMSO- $d_6$ )  $\delta$ : 28.40; 32.02; 47.20; 55.66; 114.88; 127.53; 128.12; 128.55; 128.63; 129.05; 130.96; 132.01; 134.12; 134.52; 134.59; 138.96; 141.48; 159.51; 174.15; 174.53.

**2-(2-((4'-Methoxy-[1,1'-biphenyl]-4-yl)sulfonyl)phenyl)pentanedioic acid (3b)**. The title compound was synthesized following the procedure described for the preparation of compound **3a**, starting from

diethylester **14** (411 mg, 0.804 mmol). The crude product was purified by flash chromatography (petroleum ether 40-60 °C/ EtOAc in gradient from 3:1 to EtOAc) using an Isolute Flash Si II cartridge to give the final compound **3b** as a pale-yellow powder (247 mg; 68% yield). M.p. 170°C-173°C. <sup>1</sup>H NMR (400 MHz, DMSO-*d*<sub>6</sub>) δ: 1.60-1.63 (m, 1H); 1.86-1.94 (m, 1H); 2.01-2.11 (m, 2H); 3.80 (s, 3H); 4.47 (t, *J*<sub>1</sub>= 7 Hz, 1H); 7.06-7.06 (m, AB system, 2H); 7.50- 7.52 (m, Ar, 1H); 7.60-7.62 (m, Ar, 1H); 7.66-7.72 (m, Ar, 3H); 7.83-7.90 (m, Ar, 4H); 8.18-8.20 (m, Ar, 1H); 12.28 (s, 2H). <sup>13</sup>C NMR (DMSO-*d*<sub>6</sub>) δ: 29.38; 32.39; 45.23; 55.76; 115.04; 127.53; 128.39; 128.90; 129.66; 130.47; 130.92; 134.64; 139.38; 139.49; 139.65; 145.24; 160.37; 173.72; 173.96.

**1-Hydroxy-3-(2-((4'-methoxy-[1,1'-biphenyl]-4-yl)thio)phenyl)piperidine-2,6-dione (4a).** To an ice-chilled solution of **3a** (100 mg, 0.236 mmol) in THF (1 mL) under nitrogen atmosphere, was added dropwise a solution of ethyl chloroformate (45 μL, 0.473 mmol) and *N*-methylmorpholine (0.05 mL, 0.473 mmol) in dry THF (1 mL). After stirring for 30 min at 0 °C, a precipitate of *N*-methylmorpholinium chloride was formed. In the meanwhile, a solution of hydroxylamine was prepared by adding of KOH (26.55 mg, 0.473 mmol) to a solution of NH<sub>2</sub>OH HCl (32.88 mg, 0.473 mmol) in dry methanol (0.52 mL). The mixture was stirred for 30 min at 0°C, the solid KCl was filtered off and 0.52 mL of the solution were added dropwise to the first solution containing the activated dicarboxylic acid. The final mixture was stirred for 4h at 0°C. The residue obtained from solvent evaporation was dissolved in water and extracted with EtOAc (2x25mL). The organic phase was dried over Na<sub>2</sub>SO<sub>4</sub>, filtered and brought to dryness. The crude product was purified by reverse phase flash chromatography using an Isolute Flash C18 cartridge (in gradient from CH<sub>3</sub>CN/H<sub>2</sub>O 2:1 to 1:1) and triturated with Et<sub>2</sub>O and MeOH obtaining 40.3 mg of the final compound **4a** as a white solid (40% yield). M.p. 108°C-110°C. <sup>1</sup>H NMR (400 MHz, DMSO-*d*<sub>6</sub>) δ: 1.90-1.95 (m, 1H); 2.27-2.34 (m, 1H); 2.67-2.74 (m, 1H); 2.90-2.94 (m, 1H); 3.79 (s, 3H); 4.62 (dd, *J*<sub>1</sub>=12.2 Hz, *J*<sub>2</sub>= 5 Hz, 1H); 7.02-7.03 (m, AB system, 2H); 7.27-7.44 (m, Ar, 6H); 7.58-7.61 (m, Ar, 4H); 10.04 (s, 1H). <sup>13</sup>C NMR (100 MHz,

DMSO- $d_6$ )  $\delta$ : 24.91; 32.37; 55.36; 55.66; 114.89; 127.50; 128.09; 129.02; 129.28; 130.43; 131.99; 134.13; 134.94; 135.04; 138.80; 142.06; 159.52; 168.99; 170.24.

**1-Hydroxy-3-(2-((4'-methoxy-[1,1'-biphenyl]-4-yl)sulfonyl)phenyl)piperidine-2,6-dione (4b).** To a suspension of compound **3b** (134.6 mg, 0.296 mmol) in  $\text{CH}_2\text{Cl}_2$  (2 mL), TEA (0.248 mL, 1.777 mmol), EDC (227.12 mg, 1.184 mmol), *O*-benzylhydroxylamine hydrochloride (56.74 mg, 0.355 mmol) and HOBT  $\text{H}_2\text{O}$  (1-Hydroxybenzotriazole hydrate) (160.1 mg, 1.184 mmol) were added. After the addition, the solution was stirred for 3 days at RT under inert atmosphere. The reaction mixture was washed with HCl 1N (1x25mL), water (1x25mL),  $\text{NaHCO}_3$  saturated solution (1x25mL) and brine (1x25mL). The organic phase was dried over  $\text{Na}_2\text{SO}_4$ , filtered and evaporated under low pressure. The crude product was purified by flash chromatography (*n*-hexane/ EtOAc in gradient from 6:1 to 4:1) using an Isolute Flash Si II cartridge to give the *O*-benzylic cyclic intermediate as a white powder (81 mg; 51% yield).  $^1\text{H}$  NMR (400 MHz,  $\text{CDCl}_3$ )  $\delta$ : 1.94-1.99 (m, 1H); 2.08-2.10 (m, 1H); 2.77-2.86 (m, 2H); 3.84 (s, 3H); 4.96-5.04 (m, 3H); 6.86-6.87 (m, Ar, 1H); 6.94-6.96 (m, AB system, 2H); 7.32-7.38 (m, Ar, 3H); 7.44-7.57 (m, Ar, 6H); 7.66-7.68 (m, AB system, 2H); 7.85 (d, Ar,  $J_1=8.4$  Hz, 2H); 8.15 (dd, Ar,  $J_1=6.9$  Hz,  $J_2=1$  Hz, 1H).

The *O*-benzylic cyclic intermediate (35 mg, 0.0644 mmol) was dissolved in a minimum amount of  $\text{CH}_2\text{Cl}_2$  and  $\text{BCl}_3$  (1M solution in toluene) (0.32 mL, 0.322 mmol) was added dropwise at  $0^\circ\text{C}$  under Argon atmosphere. The reaction mixture was stirred for 1h, water (0.30 mL) was added and after 15 min of stirring a precipitate formed. The aqueous phase was extracted with EtOAc (3x12mL). The product was purified by a trituration in  $\text{Et}_2\text{O}$ , affording final compound **4b** as a white powder (21 mg; 73% yield). M.p.  $108^\circ\text{C}$ - $110^\circ\text{C}$ .  $^1\text{H}$  NMR (400 MHz, DMSO- $d_6$ )  $\delta$ : 1.30-1.33 (m, 1H); 2.03-2.08 (m, 1H); 2.58-2.67 (m, 1H); 2.86-2.95 (m, 1H); 3.81 (s, 3H); 4.94 (dd,  $J_1=12.4$  Hz,  $J_2=4.2$  Hz, 1H); 7.05-7.07 (m, AB system, 2H); 7.39-7.41 (d,  $J_1=7.7$ , Ar, 1H); 7.60-7.64 (m, Ar, 1H); 7.69-7.73 (m, Ar, 3H); 7.85-7.87 (m, AB system, 2H); 7.99-8.01 (m, AB system, 2H), 8.19 (d,  $J_1=7.7$  Hz, Ar, 1H); 10.05 (s,

1H). <sup>13</sup>C NMR (100 MHz, DMSO-*d*<sub>6</sub>) δ: 25.51; 31.91; 44.78; 55.28; 114.61; 127.08; 128.11; 128.46; 128.80; 130.19; 131.60; 134.15; 138.88; 139.30; 144.82; 159.97; 168.36; 169.35.

**(2-((4'-Methoxy-[1,1'-biphenyl]-4-yl)thio)benzyl)phosphonic acid (5a).** TMSBr was added dropwise to a solution of **21** (30 mg, 0.067 mmol) in dry CH<sub>3</sub>CN (0.5 mL) cooled to 0 °C and under N<sub>2</sub> atmosphere. The reaction mixture was stirred at RT for 24h. Water was added and the mixture was stirred again for 2h at RT and extracted with CH<sub>2</sub>Cl<sub>2</sub> (5 x 25 mL). The combined organic phases were dried over Na<sub>2</sub>SO<sub>4</sub>, filtered and evaporated in vacuo to afford compound **5a** (17.7 mg; 69% yield) as a white powder. M.p. 250-254 °C; <sup>1</sup>H NMR (400 MHz, DMSO-*d*<sub>6</sub>) δ: 3.17 (s, 1H); 3.22 (s, 1H); 3.78 (s, 3H); 6.98-7.00 (m, AB system, 2H); 7.18-7.20 (m, 2H); 7.29-7.31 (m, 2H); 7.48-7.60 (m, 5H); <sup>13</sup>C NMR (100 Hz, DMSO-*d*<sub>6</sub>): δ: 55.64; 114.86; 127.44; 128.05; 130.15; 131.5; 132.10; 134.01; 135.62; 138.43; 159.43; <sup>31</sup>P NMR (161 MHz DMSO-*d*<sub>6</sub>) δ: 19.44.

**(2-((4'-Methoxy-[1,1'-biphenyl]-4-yl)sulfonyl)benzyl)phosphonic acid (5b).** A suspension of **22** (90 mg, 0.190 mmol) in a solution of HCl 12N (12 mL) was refluxed overnight. The solution was filtered and the resulting solid was dried and co-evaporated with acetone (2 x) to obtain compound **5b** as a white solid (48 mg; 60% yield). <sup>1</sup>H NMR (400 MHz, DMSO-*d*<sub>6</sub>) δ: 3.49 (d, *J*=22 Hz, 2H); 3.81 (s, 3H); 7.05-7.07 (m, AB system, 2H); 7.48-7.50 (m, 1H); 7.62-7.74 (m, 4H); 7.84-7.93 (m, 4H); 8.06-8.08 (m, 1H). <sup>13</sup>C NMR (100 MHz, DMSO-*d*<sub>6</sub>): δ: 55.75; 115.06, 127.44; 127.64; 128.33; 128.88; 130.19; 130.89; 133.14; 133.19; 133.71; 134.75, 139.40; 139.50; 139.79; 145.03; 160.36; <sup>31</sup>P NMR (161 MHz DMSO) δ: 19.28.

**2-(2-((4'-Methoxy-[1,1'-biphenyl]-4-yl)thio)phenyl)-N-(methylsulfonyl)acetamide (6a).** EDC (71.12 mg, 0.371 mmol) was added portionwise to a stirred solution of the carboxylic acid **2a** (100 mg, 0.285 mmol), DMAP (45 mg, 0.371 mmol) and methanesulfonamide (34.17 mg, 0.371 mmol) in dry CH<sub>2</sub>Cl<sub>2</sub> (2.85 mL). After stirring for 5h at RT, the mixture was washed with HCl 1N and brine. The organic phase was dried and evaporated in vacuo. The crude was then triturated twice with Et<sub>2</sub>O and *n*-

hexane to give compound **6a** as a white solid (67 mg; 55% yield). M.P: 192-194°C. <sup>1</sup>H NMR (200 MHz, CDCl<sub>3</sub>) δ: 3.14 (s, 2H); 3.84-3.85 (m, 5H); 6.94-6.99 (m, AB system, 2H); 7.23-7.51 (m, Ar, 10H); <sup>13</sup>C NMR (100 MHz, DMSO-*d*<sub>6</sub>) δ: 41.11; 41.33; 55.65; 114.88; 127.53; 128.08; 128.30; 128.45; 128.84; 128.95; 130.23; 130.31; 131.99; 132.17; 132.30; 134.27; 134.31; 134.54; 136.48; 137.13; 138.75; 159.50; 170.56.

**2-(2-((4'-Methoxy-[1,1'-biphenyl]-4-yl)sulfonyl)phenyl)-N-(methylsulfonyl)acetamide (6b).** The title compound was synthesized as previously reported for compound **6a**, starting from carboxylic acid **2b** (60 mg, 0.156 mmol). The crude product was purified by trituration with Et<sub>2</sub>O and MeOH to give **6b** as a white solid (40 mg; 56% yield). M.p. 220-224°C. <sup>1</sup>H NMR (400 MHz, DMSO-*d*<sub>6</sub>): δ 3.33 (s, 3H); 3.81 (s, 3H); 4.01 (s, 2H); 7.05-7.07 (m, AB system, 2H); 7.44 (dd, *J*<sub>1</sub>= 1.2 Hz, *J*<sub>2</sub>=7.6 Hz, 1H), 7.59 (td, *J*<sub>1</sub>=1.2 Hz, *J*<sub>2</sub>=8 Hz, 1H); 7.62-7.70 (m, 3H); 7.84-7.86 (m, AB system, 2H), 7.95-7.97 (m, AB system, 2H); 8.11 (dd, *J*<sub>1</sub>= 1.2 Hz, *J*<sub>2</sub>= 8 Hz, 1H). <sup>13</sup>C NMR (100 MHz, DMSO-*d*<sub>6</sub>): δ 41.34; 55.74; 115.07; 127.54; 128.43; 128.92; 128.97; 129.93; 130.80; 133.69; 134.16; 135.08; 139.30; 139.54; 145.29; 160.40; 170.19.

**2-(2-((4'-Methoxy-[1,1'-biphenyl]-4-yl)thio)phenyl)-N-((trifluoromethyl)sulfonyl)acetamide (7a).** EDC (57 mg, 0.297 mmol) was added portionwise to a stirred solution of the carboxylic acid **2a** (80 mg, 0.228 mmol), DMAP(36 mg; 0.320 mmol) and trifluoromethanesulfonamide (44mg; 0.297 mmol) in dry CH<sub>2</sub>Cl<sub>2</sub> (2.3 mL). After stirring for 5h at RT, the mixture was washed with HCl 1N and brine. The organic phase was dried and evaporated in vacuo. The crude was purified by flash chromatography on silica gel (CH<sub>2</sub>Cl<sub>2</sub>: MeOH in gradient from 98:2 to 95:5) to afford compound **7a** as a white solid (32.7 mg. 30% yield). M.p. 178-182°C <sup>1</sup>H NMR (200 MHz, DMSO-*d*<sub>6</sub>) δ: 3.78 (m, 5H); 7.00-7.61 (m, Ar, 12H). <sup>13</sup>C NMR (100 MHz, DMSO-*d*<sub>6</sub>) δ: 43.75; 55.64; 114.87; 118.84; 127.50; 128.09; 128.32; 128.55; 130.38; 131.86; 132.10; 133.80; 134.42; 134.84; 138.66; 138.72; 159.46; 173.45.

**2-(2-((4'-Methoxy-[1,1'-biphenyl]-4-yl)sulfonyl)phenyl)-N-((trifluoromethyl)sulfonyl)acetamide**



**(7b).** The title compound was synthesized as previously reported for compound **7a**, starting from the carboxylic acid **2b** (150mg, 0.478 mmol). After work-up, compound **7b** was obtained as a white solid (174 mg; 81% yield) without any further purification. M.p.190-193°C; <sup>1</sup>H NMR (400 MHz, DMSO-*d*<sub>6</sub>): δ 3.81 (s, 3H); 3.97 (s, 2H); 7.05-7.08 (m, AB system, 2H); 7.41 (dd, *J* = 0.8 Hz, *J* = 7.6 Hz, 1H), 7.55 (td, *J* = 1.2 Hz, *J* = 7.6 Hz, 1H); 7.63-7.70 (m, 3H); 7.82-7.84 (m, AB system, 2H), 7.90-7.92 (m, AB system, 2H); 8.08 (dd, *J* = 1.2 Hz, *J* = 7.6 Hz, 1H). <sup>13</sup>C NMR 100 MHz (DMSO-*d*<sub>6</sub>): δ 41.82; 55.73; 115.05; 121.68; 127.54; 128.34; 128.64; 128.91; 129.82; 130.90; 134.04; 134.63; 139.38; 139.45; 145.25; 160.37; 171.47. <sup>19</sup>F NMR (376 MHz, DMSO-*d*<sub>6</sub>): δ -76.92.

**1-(2-((4'-Methoxy-[1,1'-biphenyl]-4-yl)thio)phenyl)-2-(methylsulfonyl)ethanone (8a).** To a solution of dimethyl sulfone (65 mg, 0.69 mmol) in 0.52 mL of DMSO, *t*-BuOK (85 mg, 0.76 mmol), and then compound **17** (126 mg, 0.35 mmol) were added. The reaction mixture was stirred at 60 °C for 1.5h, then cooled to RT, diluted with water and acidified with 1N HCl. The precipitate was filtered, dried in vacuo and purified by flash chromatography (CHCl<sub>3</sub>) using an Isolute Flash Si II cartridge to afford **8a** as yellow solid (26 mg, 18% yield). Mp: 148-151 °C; <sup>1</sup>H NMR (400 MHz, DMSO-*d*<sub>6</sub>) δ: 3.19 (s, 3H), 3.82 (s, 3H), 5.18 (s, 2H), 6.90-6.93 (m, 1H), 7.05-7.07 (m, AB system, 2H), 7.31-7.34 (m, 1H), 7.46-7.50 (m, 1H), 7.57-7.59 (m, AB system, 2H), 7.69-7.71 (m, AB system, 2H), 7.77-7.79 (m, AB system, 2H), 8.15-8.16 (m, 1H). <sup>13</sup>C NMR (100 MHz, DMSO-*d*<sub>6</sub>) δ: 42.54, 55.69, 62.32, 114.97, 125.18, 127.86, 128.18, 128.42, 130.50, 131.70, 132.92, 133.21, 133.97, 136.01, 141.28, 143.06, 159.80, 190.70.

**1-(2-((4'-Methoxy-[1,1'-biphenyl]-4-yl)sulfonyl)phenyl)-2-(methylsulfonyl)ethanone (8b).** To a solution of dimethyl sulfone (94 mg, 0.50 mmol) in 0.38 mL of DMSO, *t*-BuOK (112 mg, 0.55 mmol), and then compound **23** (100 mg, 0.25 mmol) were added. The reaction mixture was heated at 60 °C for 1.5h, then cooled to room temperature, diluted with water and acidified with 1N HCl. The precipitate was filtered, dried in vacuo and purified by flash chromatography (CHCl<sub>3</sub>) using an Isolute Flash Si II

cartridge to afford **8b** as white solid (22 mg, 20% yield). Mp: 144-147 °C; <sup>1</sup>H NMR (400 MHz, DMSO-*d*<sub>6</sub>) δ: 3.22 (s, 3H), 3.81 (s, 3H), 5.11 (s, 2H), 7.05-7.07 (m, AB system, 2H), 7.70-7.73 (m, 3H), 7.76-7.79 (m, 1H), 7.83-7.85 (m, 1H), 7.87-7.96 (m, 4H), 8.14-8.16 (m, 1H). <sup>13</sup>C NMR (100 MHz, DMSO-*d*<sub>6</sub>) δ: 41.87, 55.31, 64.74, 114.63, 127.04, 127.24, 128.31, 128.52, 130.03, 130.32, 131.50, 134.08, 137.90, 138.52, 139.33, 145.11, 160.00, 194.42.

**Ethyl 2-(2-((4-bromophenyl)thio)phenyl)acetate (10).** To a suspension of known 2-(2-(4-bromophenylthio)phenyl)acetic acid **9**<sup>12</sup> (250 mg, 0.773 mmol) in EtOH (1 mL), SOCl<sub>2</sub> (73.16 μL, 1.005 mmol) was added dropwise. The reaction solution was refluxed for 4 h and the solvent was removed in vacuo. The residue was dissolved with water and extracted with CH<sub>2</sub>Cl<sub>2</sub> (3 x 50 mL). The combined organic phases were washed with water and brine, dried over Na<sub>2</sub>SO<sub>4</sub>, filtered and brought to dryness. The crude was purified by flash chromatography (*n*-hexane/ EtOAc in gradient from 80:1 to only EtOAc) using an Isolute Flash Si II cartridge to afford **10** as a pale-yellow oil (231.9 mg, 85% yield). <sup>1</sup>H NMR (400 MHz, CDCl<sub>3</sub>) δ: 1.2 (t, *J*<sub>H</sub> = 7.2 Hz, 3H); 3.81 (s, 2H); 4.08 (q, *J*<sub>H</sub> = 7.2 Hz, 2H); 7.00-7.03 (m, AB system, 2H); 7.24-7.29 (m, Ar, 2H); 7.31-7.37 (m, Ar, 6H).

**Ethyl 2-(2-((4'-methoxy-[1,1'-biphenyl]-4-yl)thio)phenyl)acetate (11).** A solution of Pd(OAc)<sub>2</sub> (28.19 mg, 0.125 mmol), PPh<sub>3</sub> (164.68 mg, 0.627 mmol) in EtOH (9 mL) and dry toluene (9 mL) was stirred at RT under nitrogen atmosphere for 15 min. After that period, the bromoaryl precursor **10** (1470 mg, 4.186 mmol), an aqueous solution of Na<sub>2</sub>CO<sub>3</sub> 2M (9 mL) and 4-methoxyphenylboronic acid (763 mg, 5.022 mmol) were subsequently added. The resulting mixture was refluxed at 100 °C under inert atmosphere for 2 h. Then, after cooling at room temperature, water was added and the mixture was extracted with EtOAc (3 x 125 mL). The organic phase was dried over Na<sub>2</sub>SO<sub>4</sub>, filtered and evaporated in vacuo. The obtained crude was purified by Flash chromatography (*n*-hexane: EtOAc in gradient from 50:1 to 25:1) using an Isolute Flash Si II cartridge to afford **11** as a white solid (1130 mg;

72% yield). <sup>1</sup>H NMR (400 MHz, CDCl<sub>3</sub>) δ: 1.21 (t, *J*<sub>I</sub>= 6.8 Hz, 3H); 3.84 (s, 3H); 3.86 (s, 2H); 4.10 (q, *J*<sub>I</sub>= 7.2 Hz, 2H); 6.94-6.98 (m, AB system, 2H); 7.21-7.36 (m, Ar, 5H); 7.437.50 (m, Ar, 5H).

**Diethyl 2-(2-((4'-methoxy-[1,1'-biphenyl]-4-yl)thio)phenyl)pentanedioate (12).** To a solution of **11** (494 mg, 1.306 mmol) in a mixture of *t*-BuOH/dry DMF 2:1 (9 mL), ethyl acrylate (180 μL, 1.698 mmol) was added dropwise. After being cooled to -5 °C, NaH (18.8 mg, 0.783 mmol) was added, the reaction was stirred at -5°C for 10 min and at RT for 4h. After quenching with glacial acetic acid (10 drops), Et<sub>2</sub>O was added and the organic phase was washed with water (1x50mL), NaHCO<sub>3</sub> saturated solution (1x50mL) and brine (1x50mL). The organic layer was dried over Na<sub>2</sub>SO<sub>4</sub>, filtered and evaporated under reduced pressure. The obtained crude was purified by flash chromatography (petroleum ether 40-60 °C/ EtOAc in gradient from 50:1 to 35:1) using an Isolute Flash Si II cartridge to give compound **12** as a yellow oil (365 mg; 58% yield). <sup>1</sup>H NMR (400 MHz, CDCl<sub>3</sub>) δ: 1.16 (t, *J*<sub>I</sub>=7.12 Hz, 3H); 1.23 (t, *J*<sub>I</sub>=7.12 Hz, 3H); 2.07-2.13 (m, 1H); 2.20-2.44 (m, 3H); 3.87 (s, 3H); 4.01-4.14 (m, 4H); 4.47 (t, *J*<sub>I</sub>= 7.4 Hz, 1H); 6.96-7.00 (m, AB system, 2H); 7.23-7.28 (m, Ar, 3H); 7.35 (dt, *J*<sub>I</sub>= 7.4 Hz, *J*<sub>2</sub>= 1.4 Hz, 1H); 7.43-7.51 (m, 6H).

**Ethyl 2-(2-((4'-methoxy-[1,1'-biphenyl]-4-yl)sulfonyl)phenyl)acetate (13).** To a solution of the ethyl ester **11** (186 mg, 0.492 mmol) in MeOH/THF (1:1, 11.23 mL) Oxone® (3.02 g, 9.840 mmol) and water (3.6 mL) were added using an ice-cold bath at 0°C. The reaction mixture was stirred at RT for 2 days. The organic solvents were evaporated and the aqueous layer extracted with EtOAc (3x125mL). The organic phase was dried over Na<sub>2</sub>SO<sub>4</sub>, filtered and evaporated under low pressure to give **13** as a white powder (200 mg; quantitative yields). <sup>1</sup>H NMR (CDCl<sub>3</sub>) δ: 1.16 (t, *J*<sub>I</sub>=7.1 Hz, 3H); 3.86 (s, 3H); 3.97-4.02 (m, 4H); 6.98-7.00 (m, AB system, 2H); 7.33 (dd, *J*<sub>I</sub>=7.6 Hz, *J*<sub>2</sub>= 1.1 Hz, 1H); 7.49-7.60 (m, Ar, 4H); 7.64-7.66 (m, AB system, 2H); 7.88-7.90 (m, AB system, 2H); 8.2 (dd, *J*<sub>I</sub>= 7.9 Hz, *J*<sub>2</sub>=1.3 Hz, 1H).

**Diethyl 2-(2-((4'-methoxy-[1,1'-biphenyl]-4-yl)sulfonyl)phenyl)pentanedioate (14).** The title

compound was synthesized following the procedure described above for the preparation of compound **12**, starting from ethyl ester **13** (200 mg, 0.488 mmol). After work-up, compound **14** was obtained pure as a yellow oil (241.4 mg; 97% yield). <sup>1</sup>H NMR (400 MHz, CDCl<sub>3</sub>) δ: 0.91 (t, *J*<sub>I</sub>= 7.1 Hz, 3H); 1.18 (t, *J*<sub>I</sub>=7.0 Hz, 3H); 1.90-2.00 (m, 1H); 2.103-2.147 (m, 1H); 2.31-2.38 (m, 2H); 3.77-3.90 (m, 5H); 4.03-4.09 (m, 2H); 4.64 (t, *J*<sub>I</sub>= 7.5 Hz, 1H); 6.97- 7.00 (m, AB system, 2H); 7.47-7.54 (m, Ar, 4H); 7.58-7.60 (m, Ar, 1H); 7.64-7.67 (m, AB system, 2H); 7.87-7.90 (m, AB system, 2H); 8.28 (dd, *J*<sub>I</sub>=7.9 Hz, *J*<sub>2</sub>=1.3 Hz, 1H).

**Ethyl 2-((4-bromophenyl)thio)benzoate (16).** To a suspension of known carboxylic acid **15**<sup>12</sup> (1200 mg, 3.88 mmol) in CH<sub>2</sub>Cl<sub>2</sub> (20 mL), EtOH (0.4 mL), DMAP (284 mg, 2.32 mmol), and EDC (1860 mg, 9.70 mmol) were added. The reaction mixture was stirred overnight at RT. A solution of NaHCO<sub>3</sub> saturated solution was added at the mixture was extracted with CH<sub>2</sub>Cl<sub>2</sub> (3 x 125 mL). The combined organic phases were washed with brine, dried over Na<sub>2</sub>SO<sub>4</sub>, filtered and brought to dryness. The crude was purified by flash chromatography (petroleum ether 40-60 °C/ EtOAc 50:1) using an Isolute Flash Si II cartridge to afford **16** as a white solid (1065 mg, 82% yield). <sup>1</sup>H NMR (400 MHz, CDCl<sub>3</sub>) δ: 1.41 (t, *J*<sub>I</sub>= 7.2 Hz, 3H); 4.42 (q, *J*<sub>I</sub>= 7.2 Hz, 2H); 6.82 (dd, *J* = 1.2 Hz, *J* = 8.4 Hz, Ar, 1H); 7.15 (td, , *J* = 1.2 Hz, *J* = 7.6 Hz, Ar, 1H), 7.25-7.29(m, Ar, 2H); 7.39-7.42 (m, AB system, Ar, 2H), 7.53-7.57 (m, AB system, Ar, 2H), 7.99 (dd, *J* = 1.6 Hz, *J* = 7.6 Hz, 2H).

**Ethyl 2-((4'-methoxy-[1,1'-biphenyl]-4-yl)thio)benzoate (17).** A solution of Pd(OAc)<sub>2</sub> (21.27 mg, 0.094 mmol), PPh<sub>3</sub> (124.2 mg, 0.4737 mmol) in EtOH (8 mL) and dry toluene (8 mL) was stirred at RT under nitrogen atmosphere for 15 min. Subsequently, the bromoaryl precursor **16** (1065 mg, 3.158 mmol), a solution of Na<sub>2</sub>CO<sub>3</sub> 2M (8 mL) and 4-methoxyphenylboronic acid (576 mg, 3.789 mmol) were added. The resulting mixture was refluxed at 100 °C under inert atmosphere for 2 h. After cooling at RT, water was added and the mixture was extracted with EtOAc (3 x 125mL). The organic phase was dried over Na<sub>2</sub>SO<sub>4</sub>, filtered and evaporated in vacuo. The crude was purified by flash chromatography

(Petroleum Ether 40-60 °C/ EtOAc 80:1) using an Isolute Flash Si II cartridge to give **17** as a white powder (877 mg; 76% yield). <sup>1</sup>H NMR (400 MHz, CDCl<sub>3</sub>) δ: 1.43 (t, *J*<sub>I</sub>= 7.2 Hz, 3H); 3.86 (s, 3H); 4.43 (q, *J*<sub>I</sub>= 7.2 Hz, 2H); 6.89 (d, *J*= 0.8 Hz, *J*= 8.0 Hz, 1H); 6.99-7.01 (m, AB system, 2H); 7.13 (td, *J*= 1.2 Hz, *J*= 8.0 Hz, 1H); 7.24-7.26 (m, Ar, 1H); 7.56-7.63 (m, 6H), 7.99 (dd, *J*= 1.6 Hz, *J*= 8.0 Hz, 1H).

**2-((4'-Methoxy-[1,1'-biphenyl]-4-yl)thio)benzoic acid (18)**. Ethyl ester **17** (870 mg, 2.387 mmol) was dissolved in a minimum amount of dioxane. Subsequently, NaOH 1N (12.3 mL) was added to the solution. The reaction mixture was stirred at RT for 48h. After dioxane evaporation, water was added and the mixture was acidified with HCl 1N until strongly acidic pH. The white precipitate was filtrated off and washed with water. Compound **18** was obtained as a white pearled powder without any further purification (804 mg; quantitative yield). <sup>1</sup>H NMR (400 MHz, DMSO-*d*<sub>6</sub>) δ: 3.81 (s, 3H); 6.80 (d, *J*= 0.8 Hz, *J*= 8.0 Hz, 1H), 7.04-7.06 (m, AB system, Ar, 2H); 7.22 (td, *J*= 1.2 Hz, *J*= 6.8 Hz, Ar, 1H); 7.39 (d, *J*= 1.6 Hz, *J*= 8.4 Hz, Ar, 1H); 7.56-7.58 (m, AB system, 2H) 7.68-7.70 (m, AB system, 2H); 7.74-7.76 (m, AB system, 2H); 7.92 (dd, *J*= 1.6Hz, *J*= 8 Hz, Ar, 1H).

**(2-((4'-Methoxy-[1,1'-biphenyl]-4-yl)thio)phenyl)methanol (19)**. To a solution of BH<sub>3</sub>-THF 1N (3.4 mL) carboxylic acid **18** (805 mg, 2.393 mmol) was added under inert atmosphere. The solution was stirred for 26 h at RT, then MeOH was added (4 mL) and the mixture was stirred overnight. The reaction mixture was dried, the crude was solved between NaHCO<sub>3</sub> saturated solution and CH<sub>2</sub>Cl<sub>2</sub>. The aqueous phase was extracted (3 x 50mL) with CH<sub>2</sub>Cl<sub>2</sub>. The organic layer was dried over Na<sub>2</sub>SO<sub>4</sub>, filtered and evaporated in vacuo. The obtained crude was purified by trituration with *n*-hexane to afford compound **19** (249 mg, 33% yield) as a white solid. <sup>1</sup>H NMR (400 MHz, DMSO-*d*<sub>6</sub>) δ: 3.78 (s, 3H); 4.58-4.59 (m, 2H); 5.30 (m, 1H); 7.0-7.02 (m, AB system, Ar, 2H); 7.22-7.29 (m, Ar, 4H); 7.36-7.42 (m, Ar, 1H); 7.58-7.60 (m, Ar, 5H).

**(2-(chloromethyl)phenyl)(4'-methoxy-[1,1'-biphenyl]-4-yl)sulfane (20)**. To a solution of alcohol **19**

(249 mg; 0.775 mmol) in CH<sub>2</sub>Cl<sub>2</sub> (4 mL) and pyridine (2 drops), SOCl<sub>2</sub> (73.27 μL, 1.007 mmol) was added dropwise. The mixture was stirred for 1h, and it was diluted with water. The product was extracted with Et<sub>2</sub>O (3 x 50 mL). The combined organic extracts were dried over Na<sub>2</sub>SO<sub>4</sub>, filtered and evaporated in vacuo. The crude product was purified by trituration with *n*-hexane to afford compound **20** (215 mg, 82% yield) as white powder. <sup>1</sup>H NMR (400 MHz, DMSO-*d*<sub>6</sub>) δ: 3.79 (s, 3H); 4.91 (s, 2H); 7.0-7.03 (m, AB system, 2H); 7.27-7.38 (m, 5H); 7.59-7.64 (m, 5H).

**Diethyl 2-((4'-methoxy-[1,1'-biphenyl]-4-yl)thio)benzylphosphonate (21).** A suspension of chloride **20** (100 mg, 0.293 mmol) and triethyl phosphite (2.7 mL) was stirred at 130 °C for 24 h. The reaction mixture was dissolved in Et<sub>2</sub>O (5 mL) and co-evaporated with Et<sub>2</sub>O (3 x 5mL). The crude product was purified by flash chromatography (EtOAc/*n*-hexane 5:1) using an Isolute Flash Si II cartridge to give compound **21** (68 mg; 53% yield) as a colorless oil. <sup>1</sup>H NMR (400 MHz, CDCl<sub>3</sub>) δ: 1.25 (t, *J*= 7.2Hz, 3H); 3.48 (s, 1H); 3.53 (s, 1H); 3.84 (s, 3H); 4.01-4.08 (m, 4H); 6.95-6.97 (m, AB system, 2H); 7.21-7.29 (m, 4H); 7.39-7.51 (m, 6H).

**Diethyl 2-((4'-methoxy-[1,1'-biphenyl]-4-yl)sulfonyl)benzylphosphonate (22).** To a solution of compound **21** (200 mg; 0.452 mmol) in a mixture of MeOH/THF 1:1 (4.5 mL), a solution of OXONE (1.7 g; 2.712 mmol) in water (8 mL) was added. The reaction mixture was stirred at RT overnight. The organic solvents were removed under reduced pressure, and the aqueous phase was extracted with EtOAc (3 x 50 mL). The combined organic phases were dried over Na<sub>2</sub>SO<sub>4</sub>, filtered and evaporated in vacuo. The crude product was co-evaporated with Et<sub>2</sub>O (2 x) and triturated with Et<sub>2</sub>O/*n*-hexane to afford compound **22** (191 mg; 89% yield) as a white solid. <sup>1</sup>H NMR (200 MHz, CDCl<sub>3</sub>) δ: 1.17 (t, *J*= 7.0 Hz, 6H); 3.71 (d, *J*=22.8 Hz, 2H); 3.85 (s, 3H); 3.90-4.05 (m, 4H), 6.94-7.02 (m, AB system, 2H); 7.40-7.75 (m, 7H); 7.90-7.94 (m, AB system, 2H); 8.15-8.19 (m, 1H).

**Ethyl 2-((4'-methoxy-[1,1'-biphenyl]-4-yl)sulfonyl)benzoate (23).** A solution of Oxone (2.79 g, 9.10 mmol) in water (8 mL) was slowly added to a solution of ethyl 2-((4'-methoxy-[1,1'-biphenyl]-4-

yl)thio)benzoate **17** (138 mg, 0.379 mmol) in THF/MeOH (3:1, 8 mL). The reaction was stirred at RT for 5 days, and the organic solvents were evaporated under reduced pressure. The obtained suspension was diluted with H<sub>2</sub>O, and the product was extracted with EtOAc. The combined organic extracts were dried over anhydrous Na<sub>2</sub>SO<sub>4</sub>, filtered and evaporated under reduced pressure. The crude oil was purified by flash chromatography (*n*-hexane/EtOAc 10:1) using an Isolute Flash Si II cartridge to afford **23** as a white solid (117 mg, 78% yield). <sup>1</sup>H NMR (400 MHz, CDCl<sub>3</sub>) δ: 1.39 (t, *J*=7.2 Hz, 3H), 3.85 (s, 3H), 4.45 (q, *J*=7.2 Hz, 2H), 6.97-6.99 (m, AB system, 2H), 7.51-7.57 (m, 3H), 7.61-7.63 (m, 2H), 7.66-7.69 (m, AB system, 2H), 8.01-8.04 (m, AB system, 2H), 8.13-8.15 (m, 1H).

**4.2. MMPs inhibition assays.** Recombinant human MMP-14 catalytic domain was a kind gift from Prof. Gillian Murphy (Department of Oncology, University of Cambridge, U.K.). Pro-MMP-1, pro-MMP-2 and pro-MMP-9 were purchased from Calbiochem (Merck-Millipore). Pro-MMP-12 was purchased by R&D Systems. Proenzymes were activated immediately prior to use with *p*-aminophenylmercuric acetate (2 mM APMA for 1 h at 37 °C for MMP-2, 2 mM APMA for 2 h at 37 °C for MMP-1, and 1 mM APMA for 1 h at 37 °C for MMP-9). Pro-MMP-12 was autoactivated by incubating in Fluorometric Assay Buffer (FAB: Tris 50 mM, pH 7.5, NaCl 150 mM, CaCl<sub>2</sub> 10 mM, Brij-35 0.05%, and DMSO 1%) for 30 h at 37 °C. For assay measurements, each inhibitor stock solution (DMSO, 10 mM) was further diluted in FAB at seven different concentrations. Activated enzyme (final concentrations of 0.56 nM for MMP-2, 1.3 nM for MMP-9, 1.0 nM for MMP-14cd, 2.0 nM for MMP-1, 2.3 nM for MMP-12) and inhibitor solutions were incubated in the assay buffer for 3 h at 25 °C. After the addition of 200 μM solution of the fluorogenic substrate Mca-Lys-Pro-Leu-Gly-Leu-Dap(Dnp)-Ala-Arg-NH<sub>2</sub> (Bachem) for all the enzymes in DMSO (final concentration of 2 μM for all enzymes), the hydrolysis was monitored every 10 s for 15 min, recording the increase in fluorescence ( $\lambda_{\text{ex}} = 325 \text{ nm}$ ,  $\lambda_{\text{em}} = 400 \text{ nm}$ ) with a Molecular Devices SpectraMax Gemini XPS plate reader. The assays were performed in duplicate in a total volume of 200 μL per well in 96-well microtiter plates (Corning black,

NBS). Control wells lack inhibitor. The MMP inhibition activity was expressed in relative fluorescent units (RFU). Percent of inhibition was calculated from control reactions without the inhibitor.  $IC_{50}$  was determined using the formula  $v_i/v_0 = 1/(1 + [I]/IC_{50})$ , where  $v_i$  is the initial velocity of substrate cleavage in the presence of the inhibitor at concentration  $[I]$  and  $v_0$  is the initial velocity in the absence of the inhibitor. Results were analyzed using SoftMax Pro software (version 5.4.3, Molecular Devices, Sunnyvale, CA) and Prism Software version 5.0 (GraphPad Software, Inc., La Jolla, CA).

### 4.3. Solution equilibrium studies.

**Materials and Equipment.** General analytical grade reagents were purchased from current suppliers and they were used without further purification. Potassium hydrogen phthalate ( $C_8H_5KO_4$ , p.a.) was acquired from BDH and sodium hydroxide (NaOH, p.a.) from Eka Chemicals. Dimethylsulfoxide (DMSO, dried, p.a) and potassium chloride (KCl, p.a.) were obtained from Sigma-Aldrich. Deuterated dimethylsulfoxide ( $d_6$ -DMSO, 99.9%) was purchased from Cambridge Isotope Laboratories Inc. The aqueous zinc (0.0156 M) stock solution was prepared from a 1000 ppm standard (Titrisol) and its metal content was evaluated by atomic absorption. The 0.1 M HCl solution used in calibration of the glass electrode was prepared from a Titrisol ampoule. The titrant used in pH-potentiometric and spectrophotometric titrations was prepared from carbonate free commercial concentrate (Titrisol, KOH 0.1 M ampoules). The KOH solution was standardized by titration with a solution of potassium hydrogen phthalate and was discarded whenever the percentage of carbonate, determined by Gran's method,<sup>34</sup> was greater than 0.5% of the total amount of base. The  $^1H$  NMR spectra were recorded on Bruker AVANCE III spectrometers (300 or 400 MHz).

**Potentiometric studies.** pH-potentiometric titrations of compounds **1-4 (a,b)** and **6-7 (a,b)** were accomplished in a 60% w/w DMSO/H<sub>2</sub>O medium, at  $T = 25.0 \pm 0.1$  °C and ionic strength ( $I$ ) 0.1 M KCl, by using 0.1 M KOH as titrant. Both glass and Ag/AgCl reference electrodes were previously conditioned in different DMSO/H<sub>2</sub>O mixtures of increasing DMSO % composition and the response of



the glass electrode was evaluated by strong acid – strong base (HCl/KOH) calibrations with the determination of the Nernst parameters by Gran's method. The measurements were performed in a final volume of 30.00 mL and the ligand concentrations ( $C_L$ ) were  $4-7 \times 10^{-4}$  M, under different  $C_{Zn}/C_L$  ratios: 0:1 (L), 1:1 and 1:2. All titrations were done in duplicate and under the stated experimental conditions the  $pK_w$  value (15.75) was determined and subsequently used in the computations. The stepwise protonation constants of the ligands,  $K_i = [H_iL]/[H_{i-1}L][H]$ , and the overall zinc-complex stability constants,  $\beta_{Zn_mH_hL_l} = [Zn_mH_hL_l]/[Zn]^m[H]^h[L]^l$ , were calculated by fitting the pH-potentiometric data with Hyperquad 2008 program.<sup>35</sup> The Zn(II) hydrolysis model was determined under the defined experimental conditions ( $I = 0.1$  M KCl, 60% w/w DMSO/H<sub>2</sub>O,  $T = 25.0 \pm 0.1$  °C) and the values of the stability constants ( $\log \beta_{ZnH_{-1}} = -7.02$ ,  $\log \beta_{ZnH_{-3}} = -21.76$ ) were included in the fitting of experimental data towards the equilibrium models concerned with the Zn(II)/L systems. The species distribution curves were obtained with the Hyss program.<sup>35</sup>

**<sup>1</sup>H NMR studies.** <sup>1</sup>H NMR and <sup>1</sup>H-<sup>1</sup>H COSY spectra in *d*<sub>6</sub>-DMSO were recorded for the systems L, Zn(II)/L 1:1 and Zn(II)/L 1:2 ( $C_L = 10$  mM) in the 300 and 400 MHz spectrometers.

#### 4.4. MMP crystallization experiments.

Crystallization experiments were carried out with two different constructs of the catalytic domain of MMP-12 in the presence of compounds **1b**, **2b**, **3a** and **3b**. Both carried the F171D mutation, second construct had an additional K241A mutation (Table 3S, Supporting Info). All crystals were grown by sitting drop vapor diffusion at pH 8.5 with polyethylene glycol (Table 3S) in various MMP-12 polymorphs.<sup>36</sup> Crystals of the trigonal polymorph of MMP-9 in complex with **3a** were grown with a precipitant consisting of 45% monomethyl PEG 5,000 (MPEG 5K), at pH 8.5 (Table 3S) with the use of streak seeding<sup>37</sup> with seeds from the trigonal crystal form obtained from previous studies.<sup>38</sup> This polymorph is particularly interesting as crystals often diffract at atomic resolution. All crystals were

transferred to a cryosolution and flash cooled by in liquid nitrogen. X-ray diffraction data sets were collected at the European synchrotron facility (FIP, ESRF, Grenoble, France) and at the Soleil storage ring in Saint Aubin, France, on beamlines Proxima 1 and 2A. Data for compounds **1b**, **2b** were collected using image plates while more recently data for complexes with **3a** and **3b** were collected on a Dectris Eiger 9M detector. All crystals diffracted to high resolution from good-quality diffracting crystals in three different polymorphs (Table 3S): monoclinic C2 and P2<sub>1</sub> and P2<sub>1</sub>2<sub>1</sub>2<sub>1</sub> with one molecule in the asymmetric unit for the C2 crystal form and up to four for the orthorhombic form (Table 3S). Data processing was carried out at the synchrotron facility using XDS<sup>39</sup> with the xdsme<sup>40</sup> script. Molecular replacement was carried out using MOLREP<sup>41</sup> using PDB entry 4H76 as the model followed by refinement using REFMAC5<sup>42</sup> without any ligand. The ligands restraint file was built using the smiles code in phenix.elbow<sup>43</sup> or with the monomer library sketcher from The CCP4 package.<sup>44</sup> The electron density maps were viewed and fitted in COOT.<sup>33</sup> The structures were subjected to various cycles of rebuilding and refinement with REFMAC5<sup>42</sup> and PHENIX.<sup>45</sup> The RMSD analysis was carried out using LSQKAB<sup>44</sup> and SUPERPOSE.<sup>46</sup> The figures have been made with PyMOL.<sup>47</sup>

**Supporting Information Available:** A table reporting the combustion analysis data of the final products, a table with the protonation constants of the compounds, a table with statistics for MMP-12 and MMP-9 data collection, processing and refinement (crystallographic data) and supplementary figures showing species distribution curves of compounds, superimposition of <sup>1</sup>H NMR peaks, electron density for ligands in complex with MMP-12. This material is available free of charge via the Internet at <http://pubs.acs.org>.

**PDB ID Codes:** The crystal structures for the complexes between **1b**, **2b**, and **3a,b** and MMP-12 and **3a** and MMP-9 have been deposited at the Protein Database (PDB) with the codes 6ENM, 6EOX, 6ELA, 6EKN and 6ESM, respectively. Authors will release the atomic coordinates and experimental data upon article publication.

**Acknowledgment.** The authors thank Prof. Gillian Murphy (Department of Oncology, University of Cambridge, U.K.) for the recombinant human MMP-14 catalytic domain. The help during X-ray data collection of Dr. Jean-Luc Ferrer on BM30A at the European synchrotron facility in Grenoble, France and Drs. Andrew Thomson, Gavin Fox and William Shepard and on Proxima 1 and Proxima 2A, respectively, is acknowledged with gratitude. This study was supported by funding from the University of Pisa (Progetti di Ricerca di Ateneo, PRA\_2016\_27). The authors from (IST) University of Lisboa thank the Portuguese Fundação para a Ciência e Tecnologia (FCT) for financial support to the project UID/QUI/00100/2013. Acknowledgements are also due to the Portuguese NMR (IST-UL Center) and Mass Spectrometry Networks (Node IST-CTN) for providing access to their facilities.

**Abbreviations used:** MMPI, MMP inhibitor; ECM, extracellular matrix; ZBG, zinc binding group; COPD, chronic obstructive pulmonary disease; HPD, *N*-1-hydroxypiperidine-2,6-dione; HOBT, 1-hydroxybenzotriazole; DMAP, 4-dimethylaminopyridine; EDC, *N*-(3-Dimethylaminopropyl)-*N'*-ethylcarbodiimide hydrochloride; APMA, *p*-aminophenylmercuric acetate; FAB, fluorimetric assay buffer; RFU, relative fluorescent units; SD, standard deviation; AHA, acetohydroxamic acid.

## References

---

- (1) Murphy, G.; Nagase, H. Progress in matrix metalloproteinase research. *Mol. Aspects Med.* **2008**, *29*, 290-308.
- (2) Terp, G. E.; Cruciani, G.; Christensen, I. T.; Jorgensen, F. S. Structural differences of matrix metalloproteinases with potential implications for inhibitor selectivity examined by GRID/CPCA approach. *J. Med. Chem.* **2002**, *45*, 2675-2684.
- (3) Georgiadis, D.; Dive, V. Phosphinic peptides as potent inhibitors of zinc-metalloproteases. *Top. Curr. Chem.* **2014**, *360*, 1-38.
- (4) Nuti, E.; Tuccinardi, T.; Rossello, A. Matrix Metalloproteinase inhibitors: new challenges in the era of post broad-spectrum inhibitors. *Curr. Pharm. Design* **2007**, *13*, 2087-2100.

- 
- (5) Flipo, M.; Charton, J.; Hocine, A.; Dassonneville, S.; Depez, B.; Depez-Poulain, R. Hydroxamates: relationships between structure and plasma stability. *J. Med. Chem.* **2009**, *52*, 6790-6802.
- (6) Digilio, G.; Tuccinardi, T.; Casalini, F.; Cassino, C.; Dias, D. M.; Geraldès, C. F.; Catanzaro, V.; Maiocchi, A.; Rossello, A. Study of the binding interaction between fluorinated matrix metalloproteinase inhibitors and human serum albumin. *Eur. J. Med. Chem.* **2014**, *79*, 13-23.
- (7) a) Janusz, M. J.; Hookfin, E. B.; Brown, K. K.; Hsieh, L. C.; Heitmeyer, S. A.; Taiwo, Y. O.; Natchus, M. G.; Pikul, S.; Almstead, N. G.; De, B.; Peng, S. X.; Baker, T. R.; Patel, V. Comparison of the pharmacology of hydroxamate- and carboxylate-based matrix metalloproteinase inhibitors (MMPi)s for the treatment of osteoarthritis. *Inflamm. Res.* **2006**, *55*, 60–65. b) Casalini, F.; Fugazza, L.; Esposito, G.; Cabella, C.; Brioschi, C.; Cordaro, A.; D'Angeli, L.; Bartoli, A.; Filannino, A. M.; Gringeri, C. V.; Longo, D. L.; Muzio, V.; Nuti, E.; Orlandini, E.; Figlia, G.; Quattrini, A.; Tei, L.; Digilio, G.; Rossello, A.; Maiocchi, A. Synthesis and preliminary evaluation in tumor bearing mice of new (18)F-labeled arylsulfone matrix metalloproteinase inhibitors as tracers for positron emission tomography. *J. Med. Chem.* **2013**, *56*, 2676-2689.
- (8) Roy, R.; Yang, J.; Moses, M. A. Matrix metalloproteinases as novel biomarkers and potential therapeutic targets in human cancer. *J. Clin. Oncol.* **2009**, *27*, 5287-5297.
- (9) a) Lagente, V.; Le Quement, C.; Boichot, E. Macrophage metalloelastase (MMP-12) as a target for inflammatory respiratory diseases. *Expert Opin. Ther. Targets* **2009**, *13*, 287-295. b) Molet, S.; Belleguic, C.; Lena, H.; Germain, N.; Bertrand, C. P.; Shapiro, S. D.; Planquois, J. M.; Delaval, P.; Lagente, V. Increase in macrophage elastase (MMP-12) in lungs from patients with chronic obstructive pulmonary disease. *Inflamm. Res.* **2005**, *54*, 31-36.
- (10) Newby, A. C. Matrix metalloproteinase inhibition therapy for vascular diseases. *Vascul. Pharmacol.* **2012**, *56*, 232-244

- 
- (11) a) Devel, L.; Rogakos, V.; David, A.; Makaritis, A.; Beau, F.; Cuniasse, P.; Yiotakis, A.; Dive, V. Development of selective inhibitors and substrate of matrix metalloproteinase-12. *J. Biol. Chem.* **2006**, *281*, 11152-11160. b) Dublanchet, A. C.; Ducrot, P.; Andrianjara, C.; O'Gara, M.; Morales, R.; Compère, D.; Denis, A.; Blais, S.; Cluzeau, P.; Courté, K.; Hamon, J.; Moreau, F.; Prunet, M. L.; Tertre, A. Structure-based design and synthesis of novel non-zinc chelating MMP-12 inhibitors. *Bioorg. Med. Chem. Lett.* **2005**, *15*, 3787-3790. c) Li, W.; Li, J.; Wu, Y.; Wu, J.; Hotchandani, R.; Cunningham, K.; McFadyen, I.; Bard, J.; Morgan, P.; Schlerman, F.; Xu, X.; Tam, S.; Goldman, S. J.; Williams, C.; Sypek, J.; Mansour, T. S. A selective matrix metalloprotease 12 inhibitor for potential treatment of chronic obstructive pulmonary disease (COPD): discovery of (S)-2-(8-(methoxycarbonylamino)dibenzo[b,d]furan-3-sulfonamido)-3-methylbutanoic acid (MMP408). *J. Med. Chem.* **2009**, *52*, 1799-1802.
- (12) Nuti, E.; Panelli, L.; Casalini, F.; Avramova, S. I.; Orlandini, E.; Santamaria, S.; Nencetti, S.; Tuccinardi, T.; Martinelli, A.; Cercignani, G.; D'Amelio, N.; Maiocchi, A.; Uggeri, F.; Rossello, A. Design, synthesis, biological evaluation, and NMR studies of a new series of arylsulfones as selective and potent matrix metalloproteinase-12 inhibitors. *J. Med. Chem.* **2009**, *52*, 6347-6361.
- (13) Agrawal, A.; Romero-Perez, D.; Jacobsen, J. A.; Villarreal, F. J.; Cohen, S. M. Zinc-binding groups modulate selective inhibition of MMPs. *ChemMedChem.* **2008**, *3*, 812-820.
- (14) Rouanet-Mehouas, C.; Czarny, B.; Beau, F.; Cassar-Lajeunesse, E.; Stura, E. A.; Dive, V.; Devel, L. Zinc-metalloproteinase inhibitors: evaluation of the complex role played by the zinc-binding group on potency and selectivity. *J. Med. Chem.* **2017**, *60*, 403-414.
- (15) Marques, S. M.; Tuccinardi, T.; Nuti, E.; Santamaria, S.; André, V.; Rossello, A.; Martinelli, A.; Santos, M. A. Novel 1-hydrozypiperazine-2,6-diones as new leads in the inhibition of metalloproteinases. *J. Med. Chem.* **2011**, *54*, 8289-8298.

- 
- (16) Puerta, D. T.; Griffin, M. O.; Lewis, J. A.; Romero-Perez, D.; Garcia, R.; Villarreal, F. J.; Cohen, S. M. Heterocyclic zinc-binding groups for use in next-generation matrix metalloproteinase inhibitors: potency, toxicity, and reactivity. *J. Biol. Inorg. Chem.* **2006**, *11*, 131-138.
- (17) Puerta, D. T.; Mongan, J.; Tran, B. L.; McCammon, J. A.; Cohen, S. M. Potent, selective pyrone-based inhibitors of stromelysin-1. *J. Am. Chem. Soc.* **2005**, *127*, 14148-14149.
- (18) Rossello, A.; Nuti, E.; Orlandini, E.; Balsamo, A.; Panelli, L. Inhibitors of Zinc Proteases Thioaryl Substituted and their Use. Patent WO2008015139, 2008.
- (19) Santos, M. A.; Marques, S.; Gil, M.; Tegoni, M.; Scozzafava, A.; Supuran, C. T. Protease inhibitors: synthesis of bacterial collagenase and matrix metalloproteinase inhibitors incorporating succinyl hydroxamate and iminodiacetic acid hydroxamate moieties. *J. Enzyme Inhib. Med. Chem.* **2003**, *18*, 233-242.
- (20) Nakamura, T.; Noguchi, T.; Kobayashi, H.; Miyachi, H.; Hashimoto, Y. Mono- and dihydroxylated metabolites of thalidomide: synthesis and TNF- $\alpha$  production-inhibitory activity. *Chem. Pharm. Bull.* **2006**, *54*, 1709-1714.
- (21) Park, H. I.; Jin, Y.; Hurst, D. R.; Monroe, C. A.; Lee, S.; Schwartz, M. A.; Sang, Q. X. The intermediate S1' pocket of the endometase/matrixlysin-2 active site revealed by enzyme inhibition kinetic studies, protein sequence analyses, and homology modeling. *J. Biol. Chem.* **2003**, *278*, 51646-53.
- (22) Kondo, N.; Temma, T.; Aita, K.; Shimochi, S.; Koshino, K.; Senda, M.; Iida, H. Development of matrix metalloproteinase-targeted probes for lung inflammation detection with positron emission tomography. *Sci. Rep.* **2018**, *8*, 1347.
- (23) Becker, D. P.; Barta, T. E.; Bedell, L. J.; Boehm, T. L.; Bond, B. R.; Carroll, J.; Carron, C. P.; DeCrescenzo, G. A.; Easton, A. M.; Freskos, J. N.; Funckes-Shippy, C. L.; Heron, M.; Hockerman, S.; Howard, C. P.; Kiefer, J. R.; Li, M. H.; Mathis, K. J.; McDonald, J. J.; Mehta, P. P.; Munie, G. E.;

---

Sunyer, T.; Swearingen, C. A.; Villamil, C. I.; Welsch, D.; Williams, J. M.; Yu, Y.; Yao, J. Orally active MMP-1 sparing  $\alpha$ -tetrahydropyranyl and  $\alpha$ -piperidinyl sulfone matrix metalloproteinase (MMP) inhibitors with efficacy in cancer, arthritis, and cardiovascular disease. *J. Med. Chem.* **2010**, *53*, 6653–6680.

(24) Smith, R. M.; Martell, A. E. *Critical Stability Constants*; Vol. 4, Plenum Press: New York, 1976, pp 56-57.

(25) Marques, S. M.; Abate, C.; Chaves, S.; Marques, F.; Santos, I.; Nuti, E.; Rossello, A.; Santos M. A. New bifunctional metalloproteinase inhibitors: an integrated approach towards biological improvements and cancer therapy. *J. Inorg. Biochem.* **2013**, *127*, 188-202.

(26) a) Farkas, E.; Enyedy, E.A.; Csoka, H. A comparison between the chelating properties of some dihydroxamic acids, desferrioxamine B and acetohydroxamic acid. *Polyhedron* **1999**, *18*, 2391–2398.

b) Farkas, E.; Brown, D.; Cittaro, R.; Glass, W. H. Metal complexes of glutamic acid- $\gamma$ -hydroxamic acid (Glu- $\gamma$ -ha)(N-Hydroxyglutamine) in aqueous solution. *J. Chem. Soc. Dalton Trans.* **1993**, 2803-2807.

(27) Chaves, S.; Marques, S.; Santos, M. A. Iminodiacetyl-hydroxamate derivatives as metalloproteinase inhibitors: equilibrium complexation studies with Cu(II), Zn(II) and Ni(II). *J. Inorg. Biochem.* **2003**, *97*, 345-353.

(28) Abergel, R. J.; Raymond, K. N. Terephthalamide-containing ligands: fast removal of iron from transferrin. *J. Biol. Inorg. Chem.* **2008**, *13*, 229-240.

(29) Diederichs, K.; Karplus, P. A. Better models by discarding data? *Acta Crystallogr. D. Biol. Crystallogr.* **2013**, *69*, 1215-1222.

(30) Sen, S.; Young, J.; Berrisford, J. M.; Chen, M.; Conroy, M. J.; Dutta, S.; Di Costanzo, L.; Gao, G.; Ghosh, S.; Hudson, B. P.; Igarashi, R.; Kengaku, Y.; Liang, Y.; Peisach, E.; Persikova, I.

---

Mukhopadhyay, A.; Narayanan, B. C.; Sahni, G.; Sato, J.; Sekharan, M.; Shao, C.; Tan, L.; Zhuravleva, M. A. Small molecule annotation for the Protein Data Bank. *Database* **2014**, *2014*, 1-11.

(31) Smart, O. S.; Horský, V.; Gore, S.; Svobodová Vařeková, R.; Bendová, V.; Kleywegt, G. J.; Velankar, S. Validation of ligands in macromolecular structures determined by X-ray crystallography. *Acta Crystallogr. D Struct. Biol.* **2018**, *74*, 228-236.

(32) Antoni, C.; Vera, L.; Devel, L.; Catalani, M. P.; Czarny, B.; Cassar-Lajeunesse, E.; Nuti, E.; Rossello, A.; Dive, V.; Stura, E. A. Crystallization of bi-functional ligand protein complexes. *J. Struct. Biol.* **2013**, *182*, 246-254.

(33) Emsley, P.; Lohkamp, B.; Scott, W. G.; Cowtan, K. Features and development of Coot. *Acta Crystallogr. D. Biol. Crystallogr.* **2010**, *66*, 486-501.

(34) Rossotti, F. J. C.; Rossotti, H. Potentiometric titrations using gran plots: a textbook omission. *J. Chem. Ed.* **1965**, *42*, 375-378.

(35) Gans, P.; Sabatini, A.; Vacca, A. Investigation of equilibria in solution. Determination of equilibrium constants with the HYPERQUAD suite of programs. *Talanta* **1996**, *43*, 1739-1753.

(36) Vera, L.; Antoni, C.; Devel, L.; Czarny, B.; Cassar-Lajeunesse, E.; Rossello, A.; Dive, V.; Stura, E. A. Screening using polymorphs for the crystallization of protein–ligand complexes. *Cryst. Growth Des.* **2013**, *13*, 1878-1888.

(37) Stura, E. A.; Wilson, I. A. Applications of the streak seeding technique in protein crystallization. *J. Cryst. Growth* **1991**, *110*, 270-282.

(38) Nuti, E.; Cuffaro, D.; D'Andrea, F.; Rosalia, L.; Tepshi, L.; Fabbi, M.; Carbotti, G.; Ferrini, S.; Santamaria, S.; Camodeca, C.; Ciccone, L.; Orlandini, E.; Nencetti, S.; Stura, E. A.; Dive, V.; Rossello, A. Sugar-based arylsulfonamide carboxylates as selective and water-soluble matrix metalloproteinase-12 inhibitors. *ChemMedChem.* **2016**, *11*, 1626-1637.

(39) Kabsch, W. XDS. *Acta Crystallogr. D. Biol. Crystallogr.* **2010**, *66*, 125-132.



- 
- (40) Legrand, P. XDSME: XDS Made Easier. <https://github.com/legrand/xdsme> (accessed June 8, 2016).
- (41) Vagin, A.; Teplyakov, A. Molecular replacement with MOLREP. *Acta Crystallogr. D. Biol. Crystallogr.* **2010**, *66*, 22-25.
- (42) Murshudov, G. N.; Skubák, P.; Lebedev, A. A.; Pannu, N. S.; Steiner, R. A.; Nicholls, R. A.; Winn, M. D.; Long, F.; Vagin, A. REFMAC5 for the refinement of macromolecular crystal structures. *Acta Crystallogr. D. Biol. Crystallogr.* **2011**, *67*, 355-367.
- (43) Moriarty, N. W.; Grosse-Kunstleve, R. W.; Adams, P. D. Electronic Ligand Builder and Optimization Workbench (eLBOW): a tool for ligand coordinate and restraint generation. *Acta Crystallogr. D. Biol. Crystallogr.* **2009**, *65*, 1074-1080.
- (44) Winn, M. D.; Ballard, C. C.; Cowtan, K. D.; Dodson, E. J.; Emsley, P.; Evans, P. R.; Keegan, R. M.; Krissinel, E. B.; Leslie, A. G.; McCoy, A.; McNicholas, S. J.; Murshudov, G. N.; Pannu, N. S.; Potterton, E. A.; Powell, H. R.; Read, R. J.; Vagin, A.; Wilson, K. S. Overview of the CCP4 suite and current developments. *Acta Crystallogr. D. Biol. Crystallogr.* **2011**, *67*, 235-242.
- (45) Adams, P. D.; Afonine, P. V.; Bunkóczi, G.; Chen, V. B.; Davis, I. W.; Echols, N.; Headd, J. J.; Hung, L.-W.; Kapral, G. J.; Grosse-Kunstleve, R. W.; McCoy, A. J.; Moriarty, N. W.; Oeffner, R.; Read, R. J.; Richardson, D. C.; Richardson, J. S.; Terwilliger, T.C.; Zwart, P. H. PHENIX: a comprehensive Python-based system for macromolecular structure solution. *Acta Crystallogr. D. Biol. Crystallogr.* **2010**, *66*, 213–221.
- (46) Krissinel, E.; Henrick, K. Secondary-structure matching (SSM), a new tool for fast protein structure alignment in three dimensions. *Acta Crystallogr. D. Biol. Crystallogr.* **2004**, *60*, 2256-2268.
- (47) DeLano, W. L. *The PyMOL Molecular Graphics System*; L. Schrödinger, New York Editor, 2010.

---

Table of Contents graphic

